

Exploring the versatility of human β -glucosidases and related glycosylated metabolites with novel chemical tools Bannink. S.

Citation

Bannink, S. (2025, October 24). Exploring the versatility of human β -glucosidases and related glycosylated metabolites with novel chemical tools. Retrieved from https://hdl.handle.net/1887/4281749

Version: Publisher's Version

Licence agreement concerning inclusion of doctoral

License: thesis in the Institutional Repository of the University

of Leiden

Downloaded from: https://hdl.handle.net/1887/4281749

Note: To cite this publication please use the final published version (if applicable).

Chapter 6: Summary and Future prospects

6.1 Summary

Gaucher disease (GD), one of the most well-researched inherited lysosomal storage disorders (LSDs), arises from mutations in *GBA1* alleles, leading to a deficient enzyme and subsequent build-up of its substrate, glucosylceramide (GlcCer). Nevertheless, many questions regarding GD remain unresolved, including the molecular basis for the variability in disease manifestation, the differences in severity among individual patients and the association between *GBA1* mutations and Parkinson's disease (PD). This dissertation discusses the important topic of sterol glycosides (SGs) and their relation to GBA1 and GBA2. Multiple studies suggest that GlcCer acts as a glucose donor for SG formation in animal cells. The GBA1 and GBA2 are involved in the process of transferring glucose from GlcCer to cholesterol, resulting in the formation of glucosyl cholesterol (GlcChol). There is still limited knowledge regarding the causal connection between SGs like GlcChol and many biological processes.¹ Interestingly, SGs have also been hypothesized to contribute to the development of parkinsonism.²⁻⁵

Chapter 1 gives an overview of Gaucher Disease and the related glucosyl hydrolase enzymes (GBA1, GBA2 and GBA3), highlighting the myriad pathways affected by GBA1 deficiency.⁶ It emphasizes the variability in symptom severity, which is difficult to predict based on GBA1 mutations alone.⁶ Furthermore, the chapter discusses the link between GBA1 mutations and a 20-30 fold increased risk of Parkinson's disease (PD),7 with GBA1 mutations found in 10-25% of PD patients.8 While the exact connection between GD and PD remains unclear, understanding this link could provide valuable insights into both diseases. The chapter also introduces the important topic of glycosylated metabolites (glycolites) in relation to GBA1 and GBA2 and explores the natural occurrence of sterol glucosides (SGs), 1,9,10 which are commonly found in plants, fungi, and algae. 1,9 Although no sterol glucosyltransferase (SGT) has been identified in humans, recent research suggests that GlcCer acts as a glucose donor for SG formation in animal cells. 11 GBA1 and GBA2 facilitate this process by transferring glucose from GlcCer to cholesterol, resulting in the formation of GlcChol. 11 Studies indicate that GBA2 plays the primary role in this transglucosylation, while GBA1 predominantly hydrolyses GlcChol. 11 The balance between GBA1 and GBA2 is crucial in regulating GlcChol levels, and disruptions in this equilibrium have been observed in disease models. Besides GlcChol, GBA1 also facilitates the formation of other sterol glycosides, such as galactosyl cholesterol (GalChol) and xylosyl cholesterol (XylChol), indicating a broader role in lipid metabolism.^{12,13} The ability of GBA1 and GBA2 to catalyse transglycosylation reactions suggests that additional glycosylated sterols may exist and contribute to metabolic disorders. Understanding how transglycosylation reactions are regulated within different cellular compartments is essential for determining their overall impact on health and disease.

Chapter 2 discusses how Gaucher disease (GD) diagnosis relies on GBA1 activity assays, typically using 4MU- β -Glc **1** as a fluorogenic substrate. However, these assays are hindered by background 4MU release from non-lysosomal GBA2 and cytosolic GBA3 enzymes. This chapter details the development of GBA1-selective fluorogenic substrates by synthesizing a series of 6-*O*-acyl-4MU- β -Glc derivatives with varying fatty acid chains. Due to the instability of the ester bond in lysates, alternative analogues of 6-*O*-palmitoyl-4MU- β -Glc with different chemical linkages were created. Among them, 6-*O*-alkyl-4MU- β -Glc **2**, featuring an ether linkage, proved to be the most effective GBA1 substrate, demonstrating a low K_m and a higher V_{max} compared to the ester analogue. Notably, substrate **2** was not hydrolysed by GBA2 or GBA3, making it a superior diagnostic tool for GD.

Considering that plants naturally contain glycosyl phytosterols such as campesterol, β-sitosterol, and stigmasterol, as well as 6-*O*-acyl modifications of glucose, ^{17,18} this study examined their uptake and accumulation in GD patients. Since these 6-*O*-acylglucosyl lipids could serve as GBA1 substrates, their presence was investigated in GBA1-deficient patients. LC-MS/MS analysis revealed increased levels of both 6-*O*-acylated and regular glycosylcholesterol (HexChol) in GD patient spleens, along with significant elevations in 6-*O*-acyl-glycosyl-phytosterols. This research provides the first evidence of exogenous glycolipid accumulation in GD, likely due to dietary uptake and subsequent lysosomal processing by GBA1. Given that excessive exposure to glycosylated phytosterols has been linked to Parkinson's disease (PD) in rodents, ¹⁹ further studies are needed to explore whether (6-*O*-acyl)-glycosyl-phytosterols contribute to the association between GBA1 mutations and PD risk.

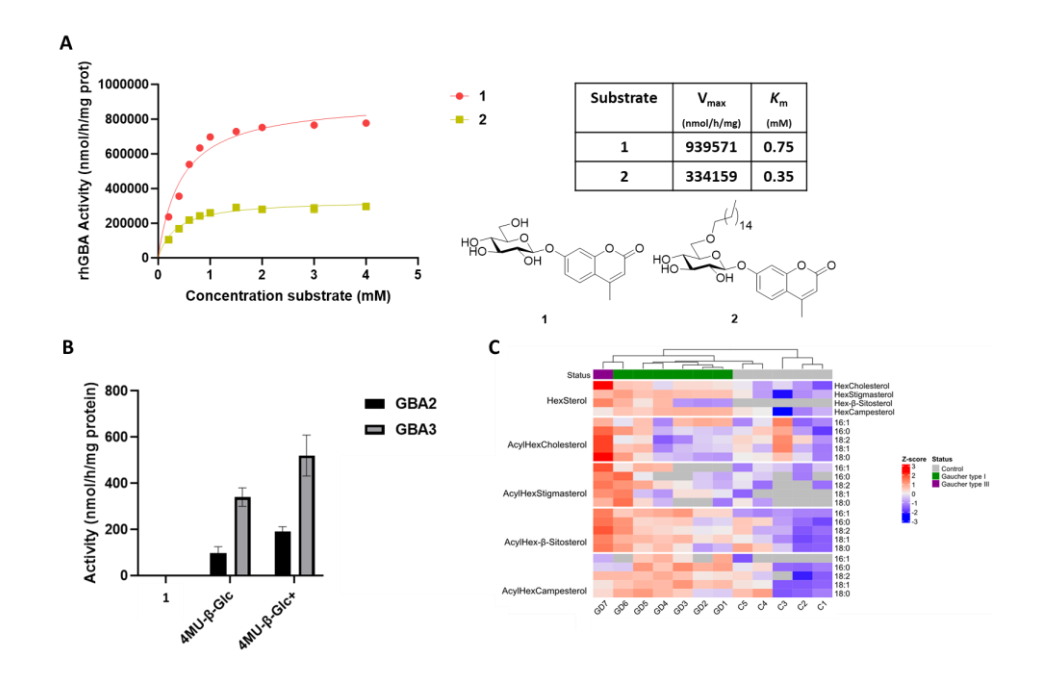


Figure 6.1: A) Chemical structures of 4MU- β -Glc **1** and 6-*O*-alkyl-4MU- β -Glc **2** and their maximum rate of hydrolysis (V_{max}) and the Michaelis constant (K_m). B) Hydrolysis of 1 mM of **2** (2.5% DMSO supplemented with 0.5% Triton X-100), 1 mM of 4MU- β -Glc **1**, and 1 mM of 4MU- β -Glc **1** + (2.5% DMSO supplemented with 0.5% Triton X-100) by HEK293T cells with either GBA2 or GBA3 OE incubated for 30 minutes at 37 °C. C) Heat map of glycosylcholesterol (HexChol) and glycosyl-stigmasterol, glycosyl- β -sitosterol, glycosyl-campesterol levels and their respective 6-*O*-acyl forms (16:0, 16:1, 18:0, 18:1 and 18:2) in spleens from non-GD and GD patients determined by LC-MS/MS analysis. Gaucher type 1, non-neuropathic variant of GD; Gaucher type 3, sub-acute neuronopathic GD case.

Chapter 3 describes the rational design of biochemical tools for identifying GBA1-produced glycolites. It examines the use of 6-O-alkyl-4MU- β -Glc 2, a GBA1-selective substrate (Chapter 2), to transglucosylate NBD-Cholesterol, a fluorescent cholesterol analogue. While effective as a glucose donor, substrate 2 exhibited a slower reaction rate than 4MU- β -Glc 1. However, it successfully facilitated *in vitro* transglucosylation of diverse metabolites, including cholesterol, desmosterol, retinol, and vitamin D₃, as confirmed by LC-MS/MS (Figure 6.2).

To improve sensitivity for detecting low-abundance metabolites, a trimethylammonium (TMA)-modified version, 6-O-alkylTMA- β -4MU- β -Glc **3**, was synthesized. Additionally, a ceramide-based analogue, 6-O-alkylTMA- β -GlcCer **4**,

was also developed to explore its physiological relevance compared to the commonly used 4MU aglycon. Kinetic analysis of the TMA-modified substrate **3** revealed similar activity to substrate **2**, though high concentrations led to reduced hydrolysis, likely due to charge interactions with sodium taurocholate. HPTLC analysis also showed that the ceramide analogue transglucosylates at a slower rate than the 4MU-based substrates. Nevertheless, modification with a C8:0 or C18:1 fatty acid could improve efficiency.²⁰

LC-MS analysis demonstrated a three-fold increase in signal intensity with the TMA handle, though fragmentation reduced this gain to ~1.5-fold. Further studies will determine if this enhancement is sufficient for identifying novel glucolites via LC-MS/MS. Optimization of MS parameters, including fragmentation patterns and solvent conditions, is ongoing. While more refinement is needed for LC-MS/MS based analysis using 6-O-alkylTMA- β -4MU- β -Glc **3** and 6-O-alkylTMA- β -GlcCer **4** as sugar donors in the transglucosylation reaction, the successful detection and quantification of 6-O-alkyl- β -GlcChol formation using substrate **2** by GBA1 transglucosylation with LC-MS/MS highlights the potential for future research. Untargeted lipidomics studies will further assess the TMA handle's utility in identifying novel GBA1-related glucolites.

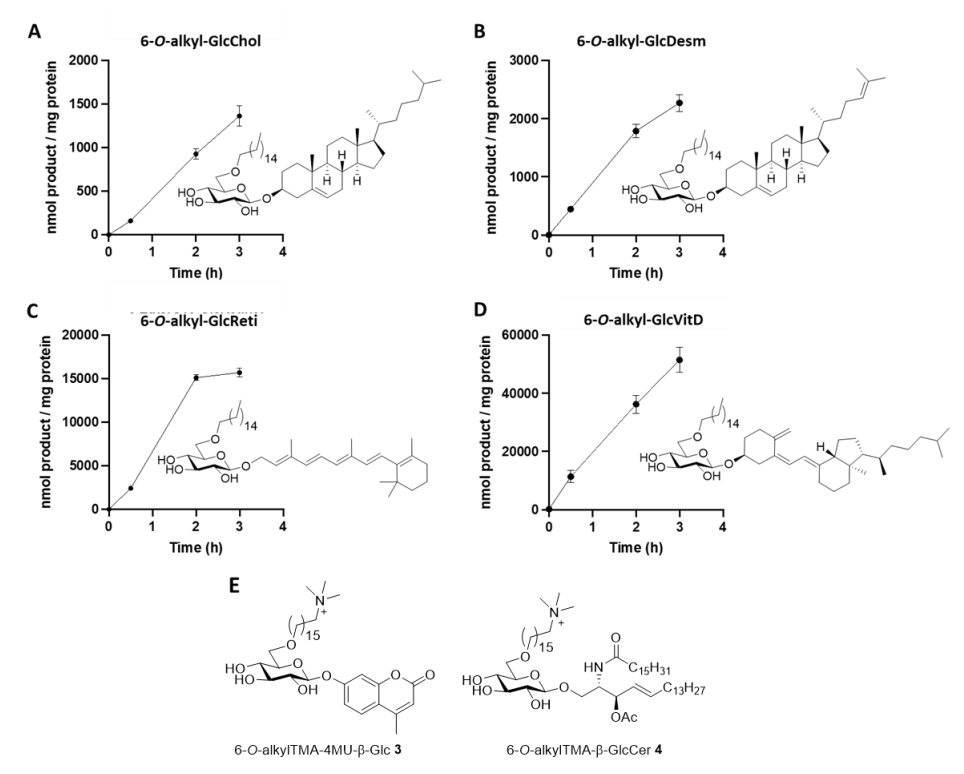


Figure 6.2: Formation of glycosylated product by rhGBA1 over time. Reaction mixtures containing 1 mM 6-O-alkyl-4MU- β -Glc (2) and 136 ng rhGBA1 (Cerezyme®) were incubated with different acceptors: A) cholesterol B) desmosterol C) retinol and D) vitamin D₃. Samples were incubated at 37 °C for 0 h, 0.5 h, 2 h and 3 h, and product formation was measured using LC-MS/MS, using $^{13}C_6$ -GlcChol as an internal standard. E) Structures of the trimethylammonium (TMA) functionalized analogues 6-O-alkylTMA-4MU- β -Glc 3 and 6-O-alkylTMA- β -GlcCer 4 bearing a trackable positive charge.

Chapter 4 attempts the synthesis and analysis of the glucosylated and galactosylated *R*- and *S*-epimers of 2-AG, along with their migrated 1-AG side products (Figure 6.3). Two synthetic routes were developed: one using acetyl protecting groups and another employing the Troc group. The acetyl route involved selective deprotection with hydrazine monohydrate but proved inconsistent, leading to loss of the arachidonic fatty acid upon scaling. To address this, a more reliable Troc-based method was tested which demonstrated superior reproducibility. Both methods ultimately yielded sufficient standards, but compounds containing the arachidonic moiety degraded within 12 months at -20

°C. Proper storage at -80 °C under argon and usage of the standards within six months is recommended in the future.

During the final silyl deprotection step, rapid migration of the arachidonic fatty acid to the secondary hydroxyl was observed. 1 H-NMR analysis in a CDCl₃/MeOD/D₂O solvent system was initially performed to track the migration of R-Gal-2-AG to R-Gal-1-AG, showing ~14% conversion to R-Gal-1-AG after 24 hours and ~30% after 70 hours. To assess migration in a biologically relevant system, LC-MS analysis was conducted in 10% DMSO/water. Over 24 hours, S-epimers exhibited higher migration (~70-60% conversion), while R-epimers showed ~40-50%. Additional experiments in 1% DMSO faced solubility issues, leading to inconsistent quantification, though migration appeared slower than in 10% DMSO. These results highlight the critical influence of solvent selection on 2-AG stability in biological studies. Solvent optimization remains crucial, as 1% DMSO proved inadequate for compound solubility, while 10% DMSO lead to reliable LC-MS analysis. Future studies are needed to explore the biological relevance of glycosylated 2-AG and 1-AG in conditions such as GD, Fabry disease, PD, and neuroinflammation.

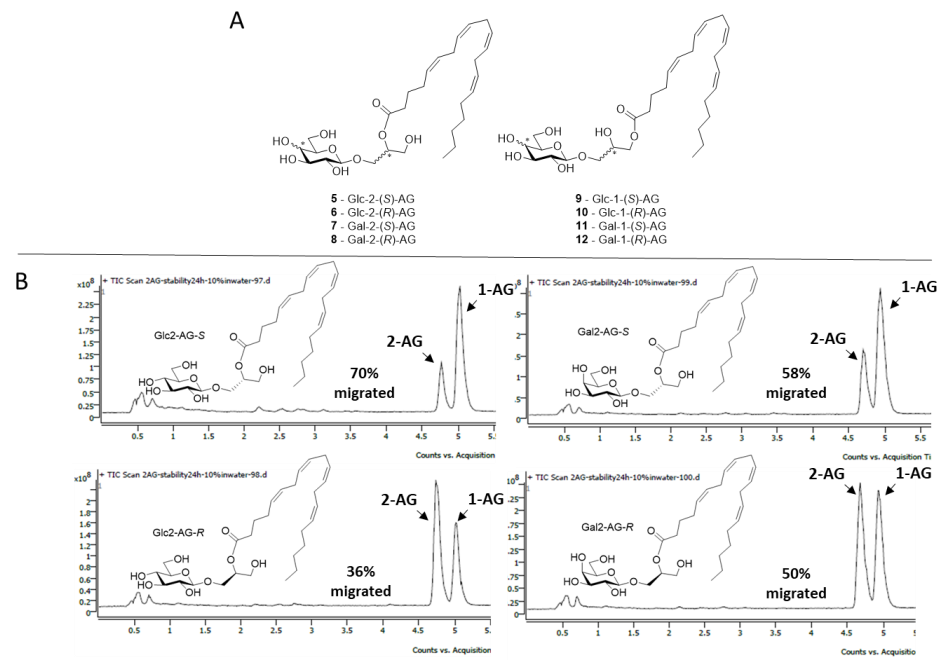


Figure 6.3: A) Chemical structures of synthesized standards of Glc- and Gal-2-AG **5-12**. B) Arachidonic fatty acid migration in the four synthesized glucosylated and galactosylated 2-AG standards after 24 h in 10% DMSO in water. LC-MS spectra using a C18 column with ammonium acetate as a counterion and a gradient of 50-90 ACN:H₂O over a total runtime of 12 minutes. Migration percentages were calculated using the 252

peak integrals obtained with the Agilent MassHunter Qualitative analysis 10.0 software.

Chapter 5 details the design of eight fluorogenic substrates, featuring a classical 4-MU or a newly designed adamantane-modified 4MU as a fluorogenic moiety (Figure 6.4). Gentiobiose based substrate 13 was designed based on unpublished results from the Schaaf lab, 21 L-Idose-based substrates 15,16,19 and 20 were inspired by studies on iminosugars as dual GCS/GBA2 inhibitors, $^{16,22-26}$ while β -D-arabinofuranose substrates 14 and 18 were designed based on GBA2-selective aziridine ABPs. 27 The addition of an adamantane lipophilic handle in substrates 17-20 was introduced with the aim of enhancing GBA2 selectivity and activity, as similar modifications have improved enzyme binding and specificity.

The 4MU- β -D-Gb substrate **13** and the 4MU- β -D-Araf substrate **14** were prepared in four and seven straightforward steps, respectively, while L-idose-based substrates **15** and **16** followed Lee *et al.*'s synthetic strategy, requiring Mitsunobu glycosylation and the separation of anomeric mixtures. The Ada4MU aglycon was synthesized from 7-hydroxycoumarin-4-acetic acid and an azido intermediate, then coupled to glucose and arabinofuranose to form substrates **17** and **18**. However, attempts to synthesize Ada4MU- β -L-idose **19** and Ada4MU- α -L-idose **20** were unsuccessful due to challenges in the Ada4MU glycosylation.

Fluorogenic substrates **13-18** were tested against rhGBA1, GBA2-overexpressing lysates and rhGBA3 or GBA3-overexpressing lysates. Whereas substrates **13-16** and **18** were not significantly hydrolysed by any of the enzymes, the Ada4MU- β -D-Glc **17** was efficiently hydrolysed by GBA1 and GBA2, similar to 4MU- β -D-Glc **1**, with minimal GBA3 activity, exhibiting GBA1/GBA2 specificity. Further work is needed to develop truly GBA2-selective substrates. Nevertheless, the study highlights that structural insights from iminosugar inhibitors and aziridine ABPs do not directly translate to substrate design probably due to conformational differences.

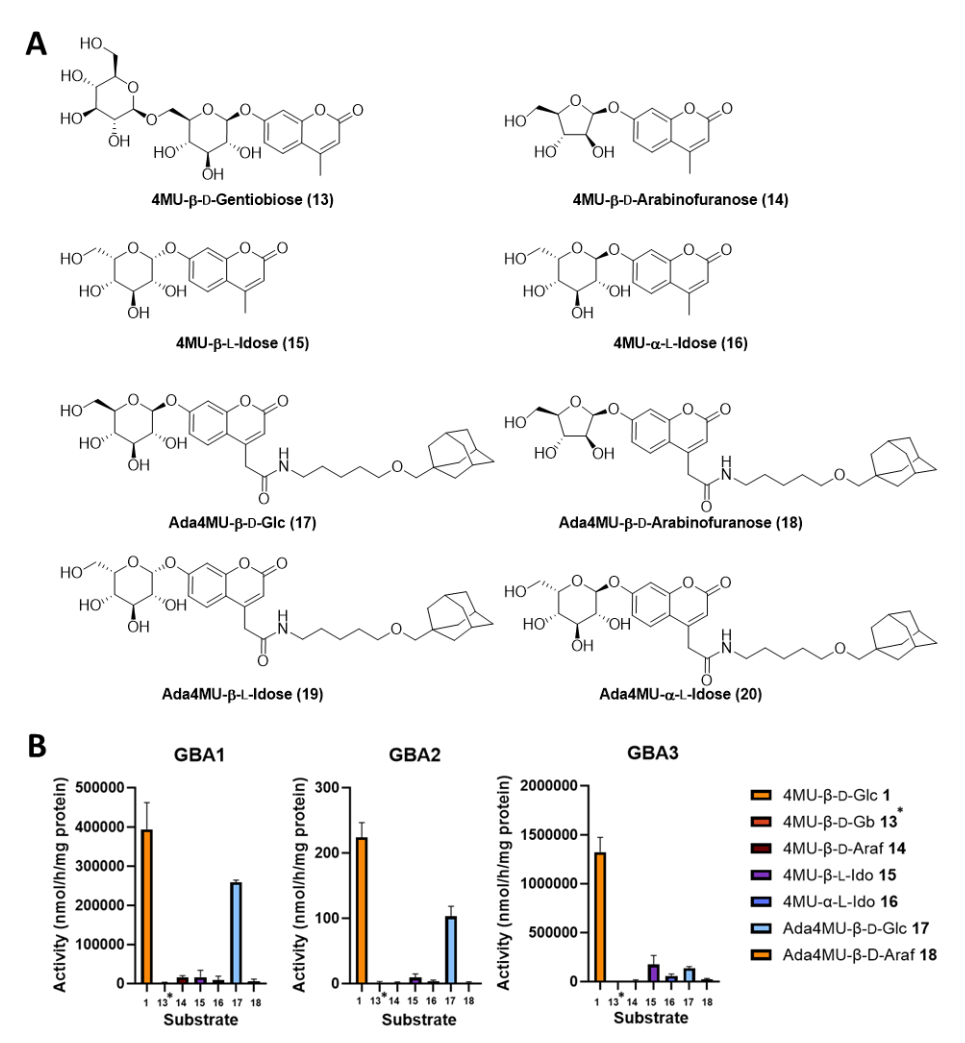


Figure 6.4: A) Chemical structures of potential GBA2 selective 4MU- and adamantly-4MU-based glycosides: 4MU-β-D-gentiobiose 13 $(4MU-\beta-D-Gb),$ 4MU-β-Darabinofuranose 14 (4MU-β-D-Araf), 4MU-β-L-idose 15 (4MU-β-L-Ido), 4MU-α-L-idose Ada4MU-β-D-glucose **17** (Ada4MU-β-D-Glc), (4MU-a-L-Ido), arabinofuranose 18 (Ada4MU-β-D-Araf), Ada4MU-β-L-idose 19 (Ada4MU-β-L-ido) and Ada4MU-α-L-idose 20 (Ada4MU-α-L-ido). B) Hydrolysis of glucosides 13-20 (at 1.5 mM) by GBA1 (rhGBA1, Cerezyme®), GBA2 (GBA2 OE and GBA1/2 KO HEK293T lysates) and GBA3 (rhGBA3) over 30 minutes. *The hydrolysis of 4MU-β-D-Gb 13 was measured at 2 mM substrate concentration and GBA3 activity was measured in GBA3 OE, GBA1/2 KO HEK293T cells lysates instead of rhGBA3.

6.2 Future prospects

Chapter 2 and 3 suggest the presence of multiple glucolites which are tied to GD besides GlcCer and GlcChol. In Chapter 2, the (6-O-acyl)-glycosyl-phytosterol levels are shown to be increased in GD spleens while Chapter 3 indicates the ability of GBA1 to glucosylate desmosterol, retinol and vitamin D₃ in vitro. These results indicate the ability of GBA1 to transglucosylate multiple metabolites and show that GBA1 has a certain degree of promiscuity in its acceptor pool. Since these data imply the possible existence of additional glycolites, further research into the presence of other metabolite acceptors is a promising avenue. The glycosylation of highly hydrophobic metabolites significantly enhances their solubility in aqueous media and their concentration in blood. For example, it has been shown that glycosylation can increase the solubility and bio-availability of certain apolar metabolites by up to 80,000-fold and 16-fold, respectively. 28,29

Since cholesterol proved to be an efficient acceptor in the transglucosylation reaction, structurally related compounds were investigated. This led to the decision to make synthetic glucosylated standards of naturally occurring and cholesterolderived estrogens: estrone (E1) and 17β-estradiol (E2) (Appendix, Scheme S6.1). 17β-Estradiol (E2), the most potent estrogen, has anti-inflammatory properties,³⁰ reducing the activation of microglia and lowering the production of proinflammatory cytokines like TNF-α and IL-6.31 In neurodegenerative diseases such as Alzheimer's³² and multiple sclerosis,³³ estrogen's anti-inflammatory effects may slow disease progression and protect against cognitive decline. 31 However, estrogen levels decline with age, particularly after menopause, which is associated with increased neuroinflammation and a higher risk of neurodegenerative conditions.³¹ The synthesis of Glc-estrone 21, Glc-estradiol 22 and ¹³C₆-Glc-estradiol 23 was pursued as illustrated in Scheme S6.1 in Appendix. These standards are currently being used to determine whether GBA1 and GBA2 can form the corresponding glucosylated products, and whether GD patients exhibit different values when compared with healthy individuals. An additional interesting similar target might be estriol (E3), a closely related estrogen which gets expressed predominantly during pregnancy.34

Figure 6.5: Chemical structures of the four tocopherols: α -Tocopherol, β -Tocopherol, γ -Tocopherol and δ -Tocopherol.

Another group of molecules identified as an interesting target is the tocopherols, which are part of the Vitamin E family. Tocopherols are a group of apolar methylated phenols, with α -tocopherol being the most biologically active form in humans. They function primarily as antioxidants, protecting cell membranes from oxidative damage by neutralizing free radicals. Tocopherols are also involved in immune function, gene expression, and cell signaling. Since α -tocopherol is the most abundant tocopherol in humans, and due to the limited commercial availability of the other tocopherols, a glucosylated standard and a ¹³C-isotope labelled analogue of α -tocopherol was synthesized following standard glycosylation and deprotection reactions (Scheme S6.2).

Emerging research continues to highlight the intricate relationship between GBA1 mutations and Parkinson's disease (PD), with α -Synuclein (α -syn) playing a central role in PD pathology. α -Synuclein (α -syn) is a 140-amino-acid protein predominantly found in the presynaptic neurons of the central nervous system.³⁶ Its structure is divided into three domains: an *N*-terminal repeat region (residues 1-87), a central non-A β component (NAC, residues 61-95) essential for aggregation, and a *C*-terminal acidic domain (residues 96-140).³⁶ In its native state, α -syn can adopt at least three conformations. In the cytosol, it likely exists as a mix of a helically folded tetramer and an unfolded monomer,³⁷ while it assumes an extended α -helical structure when bound to cellular membranes.³⁸ However, in diseased cells, α -syn forms β -sheet-rich, high-molecular-weight aggregates.³⁹ Abnormal folding and aggregation of α -syn, which causes the formation of mainly Lewy bodies, represents the pathological hallmark of PD.⁴⁰ GBA1 mutations contribute to lysosomal disfunction, which may influence α -syn aggregation.⁴¹ The lysosome-autophagy system, significantly affected by GBA1 activity in PD, plays a crucial role in regulating

α-syn levels. 42,43 Currently, three main hypotheses link GBA1 dysfunction to α-syn aggregation: (i) impaired autophagy-lysosomal breakdown results in the accumulation and aggregation of α -syn. (ii) increased accumulation of GSLs due to reduced GBA1 activity stabilizes pathogenic q-syn species, promoting their accumulation and aggregation; and (iii) improperly folded GBA1 enzyme is retained in the endoplasmatic reticulum (ER), triggering the unfolded protein response (UPR) and endoplasmic-reticulum-associated protein degradation (ERAD) pathways, prolonged activation of which leads to neuronal cell death.^{7,44,45} The most prominent hypothesis to link PD to GBA1 deficiency involves a relation between accumulation of GlcCer due to a decrease in GBA1 hydrolysis activity and α -syn aggregation. 2,46,47 It has been proven that GlcCer stabilizes toxic α -syn oligomers and subsequently interferes with ER to Golgi trafficking of GBA1.45 Interestingly, a study by Marotta et al. showed that glycosylating the threonine residue in small q-syn peptides (residues 68-77, with threonine at position 72) within the NAC region of asyn by adding N-acetyl-D-glucosamine (O-GlcNAc) reduced α-syn aggregation.⁴⁸ This could indicate that glycosylation of α-syn peptides may play a role. The synthesis of small glucosylated a-syn peptide standards and the subsequent search for these glucolites by LC-MS/MS might prove an interesting topic for future research.

Cholesterol is the most abundant sterol in mammalian cells and is known to alter the fluidity of the membrane. Furthermore, cholesterol is a constituent of lipid rafts, these are liquid-ordered regions of the plasma membrane high in cholesterol and glycosphingolipids. Importantly, these lipid rafts serve as a platform for signal transduction by selectively recruiting membrane proteins (i.e., receptors, adhesion molecules, etc.) and signalling molecules. Since GBAs influence the levels of sphingolipids, cholesterol and their glycosylated forms, these lipid rafts might also be affected in patients with deficiencies in these enzymes. Lower GCase activity is likely to have broader consequences on cell lipid composition and sphingolipid synthesis, maintenance and breakdown due to the close interrelationship between pathways of lipid metabolism and the central role played by ceramide in sphingolipid homeostasis. All the aforementioned factors should highlight the great level of interplay between multiple glucocerebrosidase enzymes, sterols, lipids and enzyme related cofactors, and indicate the level of caution that needs to be taken when doing research on these enzymes and related diseases. Se

Recently, in vitro enzyme assays have revealed that GBA1 and GBA2 can also degrade GalCer and synthesize β -GalNBD-Chol from GalCer and NBD-cholesterol (NBD-Chol, fluorescently labelled version of cholesterol used for visualization).¹³

However, GBA1 required significant amounts of recombinant enzyme as affinity of GBA1 is much higher for GlcCer when compared to GalCer.¹³ Furthermore, GalCer has not been found to accumulate within GD patients and mice samples. Interestingly, however, is the fact that GBA2 has a higher propensity towards the processing of these galactosylated metabolites (galactolites).¹³

Figure 6.6: Chemical structures of glucosyl- and galactosyl NBD-cholesterol (GlcNBD-Chol and GalNBD-Chol respectively).

Galactocyl NBD-Cholesterol (GalNBD-Chol)

Glucosyl NBD-Cholesterol (GlcNBD-Chol)

The use of detergents such as Triton-X100 can be detrimental to the enzyme activity of GBA2 and it can complicate the analysis of molecules by LC-MS. Triton-X100 is a polyethylene glycol derivative of octylphenol that acts as a non-ionic detergent (Figure 6.7), making it effective at disrupting lipid membranes while being relatively mild on proteins.⁵³ The commercial Triton-x100 consist of homologues with different numbers of ethylene oxide units, and appears on mass spectrometry analysis as an oligomer with +44 mass difference.⁵³ The LC-MS/MS data obtained in Chapter 3 was obtained in the presence of Triton-X100, which was necessary for solubilizing the modified substrates. However, the use of an alternative non-ionic detergent, as for instance C10E6, might be worth investigating for GBA2 studies.⁵⁴ Additionally, C10E6 has also been suggested to mimic the membrane environment, which might be favourable for the membrane associated GBA2 enzyme.⁵⁵ Since the use of detergents is generally undesirable and can complicate mass spectrometer data, an alternative approach would be to pursue the synthesis of less hydrophobic substrates compared to those described in Chapters 2 and 3.

Figure 6.7: Chemical structures of A) Triton X-100 and C10E6 detergents, and B) the chemical structures of fluorogenic substrates: 6-O-acyl-4MU- β -Glc derivative **24** (palmitoyl), (caproyl) derivative **25**, 6-O-alkyl-4MU- β -Glc **2**, 6-O-hexyl-4MU- β -Glc **26**, 6-O-alkylTMA-4MU- β -Glc **3**, and 6-O-hexylTMA-4MU- β -Glc **27**.

In Chapter 2, 6-O-acyl-4MU- β -Glc derivative **25** featuring a caproyl fatty acid, proved to be a GBA1-selective substrate with only slightly lower kinetics compared to the ultimately chosen palmitoyl-modified substrate **24**. Due to its significantly shorter chain length, GBA1-selective substrates derived from **25** rather than **24** might exhibit improved solubility. Specifically, the synthesis of shorter chain (hexyl) derivatives **26** and **27** could lead to fluorogenic substrates with enhanced solubility, eliminating the need for detergents.

 $6\text{-}O\text{-}Hexyl\text{-}4MU\text{-}\beta\text{-}Glc}$ linked substrate **26** could be synthesized using 1-bromohexane instead of 1-bromohexadecane in the alkylation step, following similar synthetic steps as $6\text{-}O\text{-}alkyl\text{-}4MU\text{-}\beta\text{-}Glc}$ **2**, as this route showed excellent yields and required no further optimization. For the synthesis of $6\text{-}O\text{-}hexylTMA\text{-}4MU\text{-}\beta\text{-}Glc}$ **27**, some modifications could be considered. Given that 1,6-hexanediol is significantly cheaper, this could be directly silylated, and a tosyl group could be introduced to generate the electrophile required for alkylation of the nucleophilic sugar intermediate **30**. Since the introduction of the TMA handle previously lead to compounds that were difficult to manipulate, it may be more efficient to introduce the TMA handle after glycosylation of the 4MU aglycon (Scheme 6.1).

Scheme 6.1: Proposed synthesis of 6-*O*-hexylTMA-4MU-β-Glc **27**. Reagent and conditions: a) TBSCl, imidazole, THF, rt, 16 h. b) p-TsCl, pyridine, rt. c) **29**, NaH (60% in mineral oil), DMF, rt. d) Pd/C (10%), H₂, EtOAc/EtOH 1:1, rt. e) H₂SO₄, Ac₂O/AcOH 1:1, rt. f) i. TMSBr, BiBr₃, CH₂Cl₂, 0 °C to r.t. ii. 4MU, NaOH, Acetone/H₂O (1:1), r.t., dark. g) i. NaOMe, MeOH/CH₂Cl₂, r.t. ii. TBSCl, imidazole, THF, rt. h) i. Ac₂O, pyridine, rt. ii. TBAF, THF, rt. i) i. CBr₄, PPh₃, CH₂Cl₂, rt. ii. NMe₃, MeCN, 50 °C. j) NaOMe, MeOH/CH₂Cl₂ 1:1, rt.

In addition, other quaternary ammonium salts $^{56-58}$ or quaternary phosphonium salts could be considered (Figure 6.8). 59 Fluorogenic substrates 6-*O*-hexyINAP-4MU- β -Glc **38**, 6-*O*-hexyINMI-4MU- β -Glc **39** and 6-*O*-hexyITAP-4MU- β -Glc **40** might exhibited superior ionization signals and allow for better compound detection using LC-MS/MS. These new substrates could be synthesized using building block **36**, shown in Scheme 6.1.

Figure 6.8: Proposed new substrates: 6-*O*-hexyINAP-4MU- β -Glc **38**, 6-*O*-hexyINMI-4MU- β -Glc **39** and 6-*O*-hexyITAP-4MU- β -Glc **40**.

Alternatively, the use of a 13 C isotope labelled GBA1-selective fluorogenic substrate could be considered for the discovery of novel glucolites. In addition to 13 C₆-4MU- β -Glc, which was synthesized using standard glycosylation conditions (Appendix Scheme S6.3), 13 C₆ analogues of GBA1-specific ether analogues might also be worth exploring.

In the synthesis towards the 6-O-amide-4MU-β-Glc fluorogenic substrate described in Chapter 2, a 6-N₃-4MU-β-Glc intermediate **42** was generated. This azido intermediate allows for easy functionalization with diverse alkynes using click chemistry. 6-TriazoleC16-4MU-β-Glc 43 and 6-TriazoleTMA-4MU-β-Glc 44 were synthesized and the hydrolysis of these substrates by GBA1 activity was investigated (Figure 6.9). Surprisingly, no release of 4MU was observed with substrates 43 and 44, which indicates the inability of GBA1 to process these substrates. This is in sharp contrast with O8-modified cyclophellitol-based inhibitors modified through a triazole linker, also introduced by click chemistry. These cyclophellitols functionalised with lipophilic moieties at O8 are potent and selective GBA1 inhibitors that covalently and irreversibly inhibit GBA1 by mimicking the 4H₃conformation of the koshland-double displacement mechanism.⁶⁰ Substrates 43 and 44 adopt a 4C1-conformation substrates, similar to the Michaelis complex, where the triazole modification might be detrimental for GBA1 binding in this specific conformation. This is another example where structure-activity relationships can not be simply extrapolated from glucosidase cyclophellitol-based ABPs and inhibitors to the design of substrates.

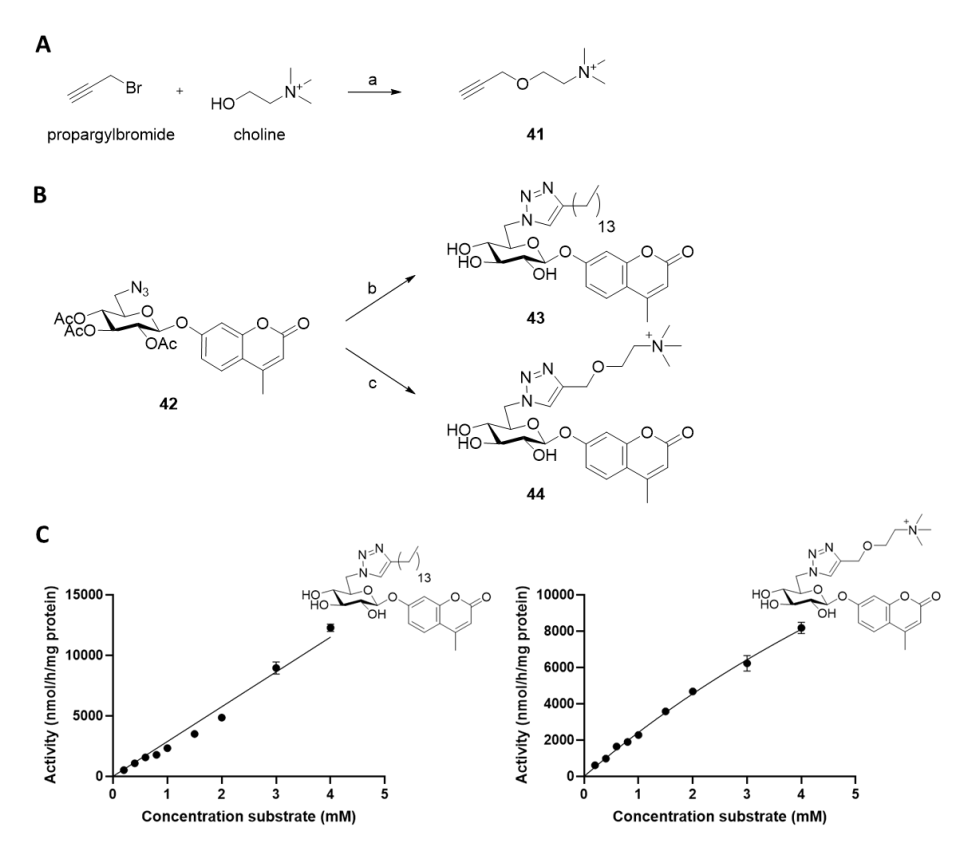


Figure 6.9: A) Synthesis towards intermediate **41** from propargylbromide and choline. B) Synthesis towards 6-TriazoleC16-4MU- β -Glc **43** and 6-TriazoleTMA-4MU- β -Glc **44** from the 6-Azido-4MU- β -Glc intermediate **42** synthesized in Chapter 2. Reagents and conditions: a) i. NaOH, ACN, 0 °C, 30 min. ii. 8 h, reflux. quantitative yield; b) i. Hexadecyne, NaAsc, CuSO₄.5H₂O, DCM/H₂O 1:1, rt., 4 h. ii. NaOMe, MeOH/CH₂Cl₂ 1:1, rt, 4 h. 61% yield 2 steps. c) i. **41**, NaAsc, CuSO₄.5H₂O, DCM/H₂O 1:1, rt., 4 h. ii. NaOMe, MeOH/CH₂Cl₂ 1:1, rt, 4 h. 40% yield 2 steps. C) Activity assays for the hydrolysis of 6-TriazoleC16-4MU- β -Glc **43** and 6-TriazoleTMA-4MU- β -Glc **44** by rhGBA1 (Cerezyme®).

While the in Chapter 5 described D-gentiobiose, D-arabinofurano and L-idose configured fluorogenic substrates **13-18** (Figure 6.4) showed no GBA2 specificity, they provided further insights into the substrate specificity for the three human glucosidases. Future research exploring different sugar configurations in combination with the Ada4MU fluorogenic moiety, such as galactose or 4-deoxy, might yield substrates with enhanced GBA2 specificity.⁵⁴

The *R*- and *S*-epimers of glucosylated and galactosylated 2- and 1- arachidonylglycerol (AG), described in Chapter 4, will aid the identification of these 262

gluco- and galactolites in complex mixtures. To enable the quantification of these metabolites, ¹³C-labelled heavy isotope standards are desirable. The synthesis of which can be achieved using the synthetic procedure outlined in Scheme 6.2. Importantly, it would be of great interest to investigate how glycosylation of 2-AG affects its binding to CB₁ and CB₂, as well as its role in the endocannabinoid system.

Scheme 6.2. Synthesis of the R- and S-epimers of the glucosylated and galactosylated 2- and 1-arachidonylglycerol. Reagent and conditions: a) i. DMAPA, THF, 0 °C-rt., 2 h. ii. TCA, Cs₂CO₃, CH₂Cl₂, rt., 4 h; b) S- or R-Solketal, BF₃·Et₂O, CH₂Cl₂, -50 °C to -30 °C, 2 h; c) Zn(NO₃)₂·(H₂O)₆, MeCN, 60 °C, 6 h; d) TBSCl, pyridine, rt., 3 h; e) i. 2,4,6-trichlorobezoylchloride, 2-arachidonic acid, Et₃N, THF, 45 min; ii. DMAP, **55-58**, THF, rt., 16 h; f) N₂H₄·H₂O, EtOH (85% in H₂O), 40 °C, 3.5 h; g) BF₃·MeCN, CH₂Cl₂, -30 °C, 1 h.

Although GD is one of the most studied LSDs, the data presented in this thesis highlights the intricate signalling and metabolic pathways involved in disease expression. It underscores the need for further investigation into metabolic dysregulation beyond GlcCer and GlcSph accumulation, the association with an increased risk of Parkinson's disease, and the interplay between GBA1 and other human glycosidases.

6.3 Chemical synthesis

6.3.1 General experimental details

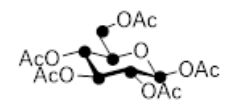
All reagents were of a commercial grade and were used as received unless stated Dichloromethane (CH₂Cl₂), tetrahydrofuran otherwise. (THF) N.Ndimethylformamide (DMF) were stored over 4 Å molecular sieves, which were dried in vacuo before use. Triethylamine and di-isopropyl ethylamine (DIPEA) were dried over KOH and distilled before use. All reactions were performed under an argon atmosphere unless stated otherwise. Solvents used for flash column chromatography were of pro analysis quality. Reactions were monitored by analytical thin-layer chromatography (TLC) using Merck aluminium sheets precoated with silica gel 60 with detection by UV absorption (254 nm) and by spraying with a solution of $(NH_4)_6Mo_7O_{24} \cdot H_2O$ (25 g/L) and $(NH_4)_4Ce(SO_4)_4 \cdot H_2O$ (10 g/L) in 10% sulfuric acid followed by charring at ~150 °C or by spraying with an aqueous solution of KMnO₄ (7%) and K₂CO₃ (2%) followed by charring at ~150 °C. Column chromatography was performed manually using either Baker or Screening Device silica gel 60 (0.04 - 0.063 mm) or a Biotage Isolera™ flash purification system using silica gel cartridges (Screening devices SiliaSep HP, particle size 15-40 µm, 60A) in the indicated solvents. ¹H-NMR and ¹³C-NMR spectra were recorded on Bruker AV-400 (400/100 MHz) and Bruker AV-I-500 (500/125 MHz) spectrometer in the given solvent. Chemical shifts are given in ppm relative to the residual solvent peak used or tetramethylsilane (TMS) as internal standard. Coupling constants are given in Hz. All given ¹³C spectra are proton decoupled. The following abbreviations are used to describe peak patterns when appropriate: s (singlet), d (doublet), t (triplet), qt (quintet), m (multiplet), br (broad), Um (4-methylumbeliferone). 2D-NMR experiments (HSQC, COSY and HMBC) were carried out to assign protons and carbons of the new structures. High-resolution mass spectra (HRMS) of intermediates were recorded with a LTQ Orbitrap (Thermo Finnigan) and final compounds were recorded with an apex-QE instrument (Bruker). LC/MS analysis was performed on an LCQ Advantage Max (Thermo Finnigan) ion-trap spectrometer (ESI+) coupled to a Surveyor HPLC system (Thermo Finnigan) equipped with a C18 column (Gemini, 4.6 mm x 50 mm, 3 µm particle size, Phenomenex) equipped with buffers A: H₂O, B: acetonitrile (MeCN) and C: 1% aqueous TFA, or an Agilent Technologies 1260 Infinity LCMS with a 6120 Quadrupole MS system equipped with buffers A: H₂O, B: acetonitrile (MeCN) and C: 100 mM NH₄OAc. For reversed-phase HPLC-MS purifications an Agilent Technologies 1200 series prep-LCMS with a 6130 Quadrupole MS system was used equipped with buffers A: 50 mM NH_4HCO_3 in H_2O and B: MeCN.

6.3.2 Synthesis and characterization data.

Synthesis of Glc-estrone 21, Glc-estradiol 22 and ${}^{13}C_6$ -Glc-estradiol 23.

The synthesis of compounds **21-23** started with the anomeric bromination of peracetylated glucose using TMS-Br and bismuth (III) bromide, which after work up of the crude, bromide was dissolved in acetone and added to a solution of either estrone or estradiol in water with cesium carbonate and tetrabutyl ammonium bromide. The peracetylated estrone intermediate could not be purified, and the mixture was immediately deprotected using sodium methoxide in a methanol and dichloromethane mixture to yield the Glc-estrone **21** standard in 2% over 3 steps after preparative HPLC purification. Similarly, the peracetylated Glc-estradiol intermediate **76** was obtained pure, in 3% yield over 3 steps. Deprotection of this intermediate using the same conditions lead to the isolation of **22** in 78% after preparative HPLC purification. For estradiol, a ¹³C isotope analogue **23** was synthesized using a ¹³C₆-Glucose for quantification purposes following similar reaction conditions.

(2S,3R,4S,5R,6R)-6-(Acetoxymethyl-¹³C)tetrahydro-2*H*-pyran-2,3,4,5-tetrayl-2,3,4,5,6-¹³C₅ tetraacetate (75)



Sodium acetate (228 mg, 2.78 mmol) was dissolved in acetic anhydride (5.24 mL, 55.5 mmol) and heated to 140 °C. ¹³C₆ D-glucose (1.00 g, 5.55 mmol) was added portion wise after which

the solution was stirred another 15 minutes at 140 °C. After the solution had attained room temperature it was poured into ice water and left until a white precipitate was collected at the bottom. The precipitate was collected by filtration and was subsequently collected and dissolved in CH_2Cl_2 . The organic layer was washed with water (2x) and brine. The water layers were extracted once more with CH_2Cl_2 and the combined organic layers were dried (MgSO₄), filtered and concentrated under reduced pressure. The crude material was then recrystallized from EtOH yielding the acetyl protected $^{13}C_6$ glucose **1** (1.42 g, 3.36 mmol, 65%) as a white powder. ^{1}H NMR (400 MHz, CDCl₃) δ 5.72 (d, J = 8.2 Hz, 1H, H-1), 5.25 (t, J = 9.5 Hz, 1H, H-3), 5.14 (t, J = 9.6 Hz, 2H, H-2 and H-4), 4.30 (dd, J = 12.5, 4.4 Hz, 1H, H-6a), 4.11 (dd, J = 12.5, 2.0 Hz, 1H, H-6b), 3.89 – 3.79 (m, 1H, H-5), 2.12 (s, 3H, CH₃-OAc), 2.09 (s, 3H, CH₃-OAc), 2.04 (s, 6H, 2xCH₃-OAc), 2.02 (s, 3H, CH₃-OAc); ^{13}C NMR (101 MHz, CDCl₃) δ 170.7, 170.2, 169.5, 169.4,

 $169.1 (5xC_q-OAc)$, 91.8 (dt, J = 48.3, 5.0 Hz, C-1), 73.4 - 72.2 (m, C-3 and C-5), 70.3 (ddd, J = 48.3, 40.8, 3.5 Hz, C-2 or C-4), 68.3 - 67.2 (m, C-2 or C-4), 61.5 (dt, J = 44.5, 4.2 Hz, C-6), $20.9, 20.8, 20.7 (5xCH_3-OAc)$; HRMS not detected.

(8R,9S,13S,14S)-13-Methyl-3-(((2S,3R,4S,5S,6R)-3,4,5-trihydroxy-6-(hydroxymethyl)tetrahydro-2H-pyran-2-yl)oxy)-6,7,8,9,11,12,13,14,15,16-decahydro-17H-cyclopenta[a]phenanthren-17-one (21)

Peracetylated glucose (200 mg, 512 μ mol) was dissolved in dry CH₂Cl₂ (5.1 mL) under protected atmosphere. The solution was cooled to 0 °C followed by the addition of TMSBr (332 μ L, 2.56 mmol) and tribromobismuthane (11.5 mg, 26

μmol). The reaction mixture was stirred for 6 hours allowing to reach room temperature. The reaction mixture was diluted with CH₂Cl₂ and washed with sat. aq. NaHCO₃ and brine. The water layers were extracted with CH₂Cl₂ and the combined organic layers were dried (MgSO₄), filtered and concentrated under reduced pressure. The crude bromide was used in the next step without further purification. Estrone (152 mg, 562 μmol) was added to a solution of Cs₂CO₃ (183 mg, 562 μmol) in water (2.6 mL). To this solution was added tetrabutylammonium bromide (16.1 mg, 50 μmol) and the bromo sugar (210 mg, 511 μmol) dissolved in acetone (2.6 mL). The mixture was stirred in the dark for 18 h at room temperature. After reaching completion the reaction was diluted with CH₂Cl₂ and washed with 1 M NaOH (3x) and brine. The water layers were extracted with CH2Cl2 and the combined organic layers were dried (MgSO4), filtered and concentrated under reduced pressure. The crude product was roughly purified by silica column chromatography to yield a mixture of the acetyl protected product 21 and excess estrone which was immediately deprotected in the next step. The impure acetyl protected sugar 21 (29 mg, 48 µmol) was dissolved in a MeOH/CH₂Cl₂ mixture (500 µL, 1:1) followed by the addition of sodium methoxide (30% in MeOH, 1 drop). The mixture was stirred for 4 hours at room temperature. After reaching completion the reaction was quenched with amberlite®, which was subsequently filtered off and washed with MeOH. The solution was concentrated yielding the crude product which was purified first by silica column chromatography followed by prep-HPLC to yield the final compound 2 (4 mg, 9 μmol, 19% yield (2% 3 steps)) as a white solid. ¹H NMR (400 MHz, MeOD) δ 7.17 (d, J = 8.1 Hz, 1H, CH-Ar), 6.83 (dd, J = 8.6, 2.7 Hz, 1H, CH-Ar), 6.77 (d, J = 2.7 Hz, 1H, CH-Ar), 4.87 – 4.83 (m, 1H, H-1), 3.86 (dd, J = 12.1, 2.5 Hz, 1H, H-6a), 3.72 (dd, J = 12.1, 4.8 Hz, 1H, H-6b), 3.49 - 3.38 (m, 4H, H-2, H-3, H-4 and H-5), 2.89 - 2.82(m, 2H, CH_2 -10'), 2.49 (dd, J = 18.6, 8.6 Hz, 1H, CH_2 -12'a), 2.37 (d, J = 10.1 Hz, 1H, CH_2 -11'a), 2.24 (d, J = 10.8 Hz, 1H, CH-7'), 2.15 (t, J = 8.8 Hz, 1H, CH₂-12'b), 2.12 – 1.95 (m, 2H, $2xCH_2$ -15'a and 9'a), 1.90 (dd, J = 9.1, 2.5 Hz, 1H, CH_2 -16'a), 1.71 - 1.33 (m, 6H, CH_2 -8, CH-14', $4xCH_2$ -b), 0.90 (s, 3H, CH_3); ^{13}C NMR (101 MHz, MeOD) δ 155.9, 138.3, 134.4 ($3xC_q$ -Ar), 126.7, 117.2, 114.6 (3xCH-Ar), 101.5 (C-1), 77.0, 76.8, 73.9, 70.5 (C-2, C-3, C-4 and C-5), 62.0 (C-6), 50.8 (CH_2 -14'), 44.5 (CH_2 -7'), 38.7 (CH_2 -8'), 36.3 (CH_2 -12'), 31.9 (CH_2 -16'), 30.0 (CH_2 -10'), 26.9 (CH_2 -9'), 26.3 (CH_2 -11'), 21.9 (CH_2 -15'), 14.1 (CH_3); HRMS: calcd. for C_2 4 H_3 2 O_7 [CH_2 1+30, 24863, found: 450,24938.

(2*R*,3*R*,4*S*,5*R*,6*S*)-2-(Acetoxymethyl)-6-(((8*R*,9*S*,13*S*,14*S*,17*S*)-17-hydroxy-13-methyl-7,8,9,11,12,13,14,15,16,17-decahydro-6*H*-cyclopenta[a]phenanthren-3-yl)oxy)tetrahydro-2*H*-pyran-3,4,5-triyl triacetate (76)

Peracetylated glucose (200 mg, 512 μ mol) was dissolved in dry CH₂Cl₂ (5.1 mL) under protected atmosphere. The solution was cooled to 0 °C followed by the addition of TMSBr (332 μ L, 2.56 mmol) and tribromobismuthane (11.5 mg, 26

μmol). The reaction mixture was stirred for 6 hours allowing to reach room temperature. The reaction mixture was diluted with CH₂Cl₂ and washed with sat. aq. NaHCO₃ and brine. The water layers were extracted with CH₂Cl₂ and the combined organic layers were dried (MgSO₄), filtered and concentrated under reduced pressure. The crude bromide was used in the next step without further purification. Estradiol (199 mg, 730 μmol) was added to a solution of Cs₂CO₃ (237 mg, 730 μmol) in water (2.4 mL). To this solution was added tetrabutylammonium bromide (16.1 mg, 50 μmol) and the bromo sugar (210 mg, 511 µmol) dissolved in acetone (2.4 mL). The mixture was stirred in the dark for 18 h at room temperature. After reaching completion the reaction was diluted with CH₂Cl₂ and washed with 1 M NaOH (3x) and brine. The water layers were extracted with CH₂Cl₂ and the combined organic layers were dried (MgSO₄), filtered and concentrated under reduced pressure. The product was purified by silica column chromatography yielding the product (17 mg, 28 µmol, 6% yield over 2 steps) as a white solid. ¹H NMR (400 MHz, CDCl₃) δ 7.20 (d, J = 8.1 Hz, 1H, CH-Ar), 6.77 (dd, J = 8.6, 2.7 Hz, 1H, CH-Ar), 6.71 (d, J = 2.7 Hz, 1H, CH-Ar), 5.33 – 5.20 (m, 2H, H-2 and H-3), 5.15 (t, J =9.5 Hz, 1H, H-4), 5.04 (d, J = 7.6 Hz, 1H, H-1), 4.27 (dd, J = 12.3, 5.3 Hz, 1H, H-6a), 4.17 (dd, J = 12.2, 2.4 Hz, 1H, H-6b), 3.85 (ddd, J = 10.0, 5.3, 2.5 Hz, 1H, H-5), 3.73 (t, J = 8.5)Hz, 1H, H-17'), 2.89 - 2.79 (m, 2H, CH₂-10'), 2.30 (dd, J = 13.5, 3.5 Hz, 1H, CH₂-11'a), 2.24– 2.10 (m, 2H, CH-7' and CH₂-16'a), 2.08 (s, 3H, CH₃-OAc), 2.05 (s, 3H, CH₃-OAc), 2.04 (s, 3H, CH₃-OAc), 2.03 (s, 3H, CH₃-OAc), 1.95 (dt, J = 12.7, 3.2 Hz, 1H, CH₂-12'a), 1.88 (ddd, J = 9.8, 5.7, 2.9 Hz, 1H, CH₂-9'a), 1.70 (ddd, <math>J = 13.4, 10.8, 4.6 Hz, 1H, CH₂-15'a), 1.55 - 1.29(m, 7H, CH-8', CH-14, 5xCH₂-b), 0.77 (s, 3H, CH₃); 13 C NMR (101 MHz, CDCl₃) δ 170.8,

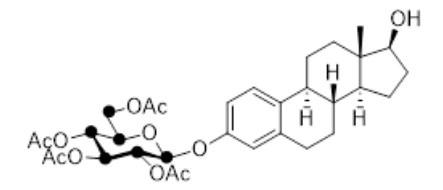
170.4, 169.6, 169.5 ($4xC_q$ -OAc), 154.9, 138.4, 135.6 ($3xC_q$ -Ar), 126.6, 117.1, 114.4 (3xCH-Ar), 99.4 (C-1), 82.0 (C-17), 72.9 (C-2 or C-3), 72.1 (C-5), 71.3 (C-2 or C-3), 68.5 (C-4), 62.2 (C-6), 50.1 (C-14'), 44.1 (C-7'), 43.4 (C-16'), 38.8 (C-8'), 36.8 (C-12'), 30.7 (C-10'), 27.2 (C-9'), 26.4 (C-11'), 23.2 (C-15'), 20.9, 20.80, 20.78, 20.75 ($4xCH_3$ -OAc), 11.2 (CH₃); HRMS: calcd. for $C_{32}H_{42}O_{11}$ [M+NH₄] $^+$ 620,30654, found: 620,30700.

(2*S*,3*R*,4*S*,5*S*,6*R*)-2-(((8*R*,9*S*,13*S*,14*S*,17*S*)-17-Hydroxy-13-methyl-7,8,9,11,12,13,14,15,16,17-decahydro-6*H*-cyclopenta[a]phenanthren-3-yl)oxy)-6-(hydroxymethyl)tetrahydro-2*H*-pyran-3,4,5-triol (22)

The acetyl protected sugar **76** (16 mg, 27 μ mol) was dissolved in a MeOH/CH₂Cl₂ mixture (250 μ L, 1:1) followed by the addition of sodium methoxide (30% in MeOH, 1 drop). The mixture was stirred for 4 hours at room temperature.

After reaching completion the reaction was quenched with amberlite®, which was subsequently filtered off and washed with MeOH. The solution was concentrated yielding the crude product which was purified first by silica column chromatography followed by prep-HPLC to yield the final compound **22** (9 mg, 21 μ mol, 78% yield) as a white solid. 1 H NMR (400 MHz, MeOD) δ 7.17 (d, J = 8.8 Hz, 1H, CH-Ar), 6.81 (dd, J = 8.6, 2.7 Hz, 1H, CH-Ar), 6.75 (d, J = 2.6 Hz, 1H, CH-Ar), 4.86 – 4.83 (m, 1H, H-1), 3.86 (dd, J = 12.1, 2.5 Hz, 1H, H-6a), 3.72 (dd, J = 12.1, 4.8 Hz, 1H, H-6b), 3.64 (t, J = 8.6 Hz, 1H, CH-17'), 3.51 – 3.37 (m, 4H, H-2, H-3, H-4 and H-5), 2.84 – 2.74 (m, 2H, CH₂-10'), 2.31 – 2.22 (m, 1H, CH₂-11'a), 2.19 – 2.10 (m, 1H, CH-7'), 2.08 – 1.97 (m, 1H, CH₂-16'a), 1.93 (dt, J = 12.4, 3.3 Hz, 1H, CH₂-12'a), 1.89 – 1.81 (m, 1H, CH₂-9'a), 1.71 – 1.61 (m, 1H, CH₂-15'a), 1.53 – 1.10 (m, 7H, CH-8', CH-14', 5xCH₂-b), 0.74 (s, 3H, CH₃); 13 C NMR (101 MHz, MeOD) δ 155.7, 138.5, 135.2 (3xC_q-Ar), 126.7, 117.2, 114.5 (3xCH-Ar), 101.6 (C-1), 81.8 (C-17'), 77.0, 76.8, 73.9, 70.5 (C-2, C-3, C-4 and C-5), 62.0 (C-6), 50.5 (C-14'), 44.5 (C-7'), 43.6 (C-16'), 39.3 (C-8'), 37.1 (C-12'), 30.2 (C-10'), 27.7 (C-9'), 26.8 (C-11'), 23.5 (C-15'), 11.4 (CH₃); HRMS: calcd. for C₂4H₃4O7 [M+NH₄]+ 452,26428, found: 452,26453.

(2R,3R,4S,5R,6R)-2-(Acetoxymethyl-¹³C)-6-(((8R,9S,13S,14S,17S)-17-hydroxy-13-methyl-7,8,9,11,12,13,14,15,16,17-decahydro-6H-cyclopenta[a]phenanthren-3-yl)oxy)tetrahydro-2H-pyran-3,4,5-triyl-2,3,4,5,6-¹³C₅ triacetate (77)



Peracetylated $^{13}C_6$ glucose (205 mg, 518 µmol) was dissolved in dry CH₂Cl₂ (5.3 mL) under protected atmosphere. The solution was cooled to 0 °C followed by the addition of Hydrogen bromide (33% in acetic acid, 864 µL, 5.3 mmol)

The reaction mixture was stirred for 3 hours on ice. The reaction mixture was diluted with CH₂Cl₂ and washed with ice water, sat. aq. NaHCO₃ and brine. The water layers were extracted with CH2Cl2 and the combined organic layers were dried (MgSO4), filtered and concentrated under reduced pressure. The crude bromide was used in the next step without further purification. Estradiol (157 mg, 575 µmol) was added to a solution of Cs₂CO₃ (187 mg, 575 µmol) in water (2.6 mL). To this solution was added tetrabutylammonium bromide (17 mg, 52 µmol) and the bromo sugar (215 mg, 516 µmol) dissolved in acetone (2.6 mL). The mixture was stirred in the dark for 18 h at room temperature. After reaching completion the reaction was diluted with CH2Cl2 and washed with 1 M NaOH (3x) and brine. The water layers were extracted with CH₂Cl₂ and the combined organic layers were dried (MgSO₄), filtered and concentrated under reduced pressure. The product was purified by silica column chromatography yielding the product **77** (11 mg, 18 µmol, 3% yield over 2 steps) as a white solid. ¹H NMR (400 MHz, CDCl₃) δ 7.20 (d, J = 8.6 Hz, 1H, CH-Ar), 6.77 (dd, J = 8.6, 2.7 Hz, 1H, CH-Ar), 6.71 (d, J = 2.6 Hz, 1H, CH-Ar), 5.25 (q, J = 9.3, 8.7 Hz, 2H, H-2 and H-3), 5.15 (t, J = 9.1 Hz, 1H, H-4), 5.03 (d, J = 7.0 Hz, 1H, H-1), 4.26 (dd, J = 12.1, 5.1 Hz, 1H, H-6a), 4.22 – 4.14 (m, 1H, H-6b), 3.84 (d, J = 10.1 Hz, 1H, H-5), 3.73 (t, J = 8.2 Hz, 1H, H-17'), 2.87 – 2.79 (m, 2H, CH_2-10'), 2.28 (t, J = 3.5 Hz, 1H, CH_2-11' a), 2.23 - 2.13 (m, 1H, CH-7' and CH_2-16' a), 2.08 (s, 2H, CH₃-OAc), 2.05 (s, 3H, CH₃-OAc), 2.04 (s, 3H, CH₃-OAc), 2.03 (s, 2H, CH₃-OAc), 1.95 (dt, J = 12.5, 3.3 Hz, 1H, CH₂-12'a), 1.88 (ddt, J = 11.4, 5.7, 2.5 Hz, 1H, CH₂-9'a), 1.75 – 1.65 (m, 1H, CH₂-15'a), 1.55 – 1.26 (m, 7H, CH-8', CH-14', 5xCH₂-b), 0.77 (s, 3H, CH₃); ¹³C NMR (101 MHz, CDCl₃) δ 170.7, 170.3, 169.6, 169.5 (4xC_q-OAc), 138.3, 135.6 (3xC_q-Ar), 126.7, 117.1, 114.4 (3xCH-Ar), 99.34 (dt, J = 48.4, 5.1 Hz, C-1), 82.1 (C-17'), 73.4 – 70.7 (m, C-2, C-3 and C-5), 68.4 (td, J = 41.2, 3.8 Hz, C-4), 62.17 (dt, J = 44.7, 4.3 Hz, C-6), 50.2(C-14'), 44.0 (C-7'), 43.3 (C-16'), 38.8 (C-8'), 36.8 (C-12'), 30.6 (C-10'), 27.1 (C-9'), 26.3 (C-10'), 27.1 (C-9'), 26.3 (C-10'), 27.1 (C-9'), 27.1 11'), 23.2 (C-15'), 20.9, 20.80, 20.79, 20.76 (4xCH₃-OAc), 11.2 (CH₃); HRMS: not detected

(2R,3R,4S,5S,6R)-2-(((8R,9S,13S,14S,17S)-17-Hydroxy-13-methyl-7,8,9,11,12,13,14,15,16,17-decahydro-6*H*-cyclopenta[a]phenanthren-3-yl)oxy)-6-(hydroxymethyl- 13 C)tetrahydro-2*H*-pyran-3,4,5-triol-2,3,4,5,6- 13 C₅ (23)

The acetyl protected $^{13}C_6$ sugar **77** (11 mg, 18 μ mol) was dissolved in a MeOH/CH $_2$ Cl $_2$ mixture (400 μ L, 1:1) followed by the addition of sodium methoxide (30% in MeOH, 1 drop). The mixture was stirred for 4 hours at room temperature.

After reaching completion the reaction was quenched with amberlite®, which was subsequently filtered off and washed with MeOH. The solution was concentrated yielding the crude product which was purified first by silica column chromatography followed by prep-HPLC to yield the final compound 23 (6 mg, 14 µmol, 76% yield) as a white solid. ¹H NMR (400 MHz, MeOD) δ 7.51 (s, 1H, OH-17), 7.16 (d, J = 8.6 Hz, 1H, CH-Ar), 6.82 (dd, J = 8.6, 2.7 Hz, 1H, CH-Ar), 6.75 (d, J = 2.6 Hz, 1H, CH-Ar), 4.84 (d, J = 7.0Hz, 1H, H-1), 3.85 (dd, J = 12.0, 2.2 Hz, 1H, H-6a), 3.72 (dd, J = 12.0, 4.5 Hz, 1H, H-6b), 3.64 (t, J = 8.6 Hz, 1H, H-17'), 3.49 – 3.36 (m, 4H, H-2, H-3, H-4 and H-5), 2.84 – 2.76 (m, 2H, CH_2-10'), 2.27 (dd, J = 13.5, 3.6 Hz, 1H, $CH_2-11'a$), 2.14 (td, J = 11.0, 4.1 Hz, 1H, $CH_2-11'a$) 7'), 2.02 (dtd, J = 13.2, 9.3, 5.6 Hz, 1H, CH₂-16'a), 1.93 (dt, J = 12.6, 3.3 Hz, 1H, CH₂-12'a), 1.88 - 1.81 (m, 1H, CH₂-9'a), 1.73 - 1.60 (m, 1H, CH₂-15'a), 1.53 - 1.11 (m, 7H, CH-8', CH-14', 5xCH₂-b), 0.74 (s, 3H, CH₃); 13 C NMR (101 MHz, MeOD) δ 155.8, 138.5, 135.3 (3xC_g-Ar), 126.7, 117.3, 114.5 (3xCH-Ar), 101.6 (dt, J = 47.0, 4.5 Hz, C-1), 77.5 – 76.1 (m, $2x^{13}C_6$), 73.9 (ddd, J = 47.0, 39.3, 2.4 Hz, ${}^{13}C_{6}$), 70.5 (ddd, J = 41.5, 39.3, 2.4 Hz, ${}^{13}C_{6}$), 62.0 (dt, J = 41.5), 63.1 (ddd, J = 41.5), 63.1 (ddd, J = 41.5), 63.2 (ddd, J = 41.5), 63.3 (ddd, J = 41.542.8, 4.0 Hz, C-6), 50.5 (C-14'), 44.5 (C-7'), 43.5 (C-16'), 39.4 (C-8'), 37.2 (C-12'), 30.1 (C-10'), 27.7 (C-9'), 26.8 (C-11'), 23.5 (C-15'), 11.4 (CH₃); HRMS: calcd. for C₁₈¹³C₆H₃₄O₇ [M+NH₄]⁺: 458.28441, Found: 458.28521.

Synthesis of ${}^{12}C_6$ and ${}^{13}C_6$ glucosylated a-tocopherol standards **79** and **81**.

The synthesis of the glucosylated α -tocopherol standards started with the preparation of both the 12 C and 13 C benzoyl protected glucose-configured imidate donors using standard conditions as described in Chapter 2. Glucosylated intermediates **78** and **80** were both obtained in 90% yield, which after deprotection of the benzoyl protecting groups lead to the desired Glc- α -Tocopherol **79** and 13 C₆-Glc- α -Tocopherol **81** in 88% and 76%, respectively.

(2R,3R,4S,5R,6S)-2-((Benzoyloxy)methyl)-6-(((R)-2,5,7,8-tetramethyl-2-((4R,8R)-4,8,12-trimethyltridecyl)chroman-6-yl)oxy)tetrahydro-2H-pyran-3,4,5-triyl tribenzoate (78)

The bezoyl protected imidate glucose donor (100 mg, 135 μ mol) was dissolved in anhydrous CH₂Cl₂ (2.7 mL) and

α-Tocopherol (87 mg, 202 μmol) was added. The reaction mixture was cooled to −30 °C on activated 4 Å molecular sieves under argon atmosphere. Boron trifluoride etherate (7 µL, 54 µmol) was added and stirring was maintained for 5 hours. After completion the reaction was neutralized with triethylamine (18 µL) and filtered over celite after which the mixture was evaporated under reduced pressure and purified by silica column chromatography to yield the product 7 (123 mg, 122 µmol, 90%) as a white solid. 1 H NMR (400 MHz, CDCl₃) δ 8.05 – 8.00 (m, 2H, 2xCH-OBz), 7.97 – 7.83 (m, 6H, 6xCH-OBz), 7.58 – 7.28 (m, 12H, 12xCH-OBz), 6.01 – 5.87 (m, 2H), 5.75 (t, J = 9.5 Hz, 1H), 5.09 (d, J = 7.6 Hz, 1H), 4.59 (dt, J = 12.0, 3.4 Hz, 1H), 4.41 (ddd, J = 12.012.0, 5.2, 3.2 Hz, 1H), 3.99 (ddd, J = 9.9, 5.2, 3.2 Hz, 1H), 2.53 – 2.43 (m, 2H), 2.13 (d, J = 3.3 Hz, 3H), 2.09 (d, J = 2.7 Hz, 3H), 2.02 (s, 3H), 1.73 (ddg, J = 19.6, 12.9, 6.6 Hz,2H), 1.57 - 1.02 (m, 21H), 0.90 - 0.81 (m, 12H); 13 C NMR (101 MHz, CDCl₃) δ 166.2, 166.0, 165.3, 165.2 (4xC₀-OBz), 148.7, 145.5 (2xC₀-tocopherol), 133.6, 133.4, 133.2, 130.0, 130.0, 129.8 (10xCH-OBz), 129.3, 128.9 (2xC₀-tocopherol), 128.5, 128.4 (10xCH-OBz), 123.0, 117.6 $(2xC_a-tocopherol)$, 102.6 (C-1), 75.0 $(C_a-tocopherol)$, 73.3 (C-3), 72.4 (C-2), 72.2 (C-5), 69.9 (C-4), 63.0 (C-6), 40.3, 39.5, 37.5 (3xCH₂-alkyl), 32.8 (CH-alkyl), 31.3 (CH₂-tocopherol), 28.2 (CH-tocopherol), 24.9, 24.6 (2xCH₂-alkyl), 23.8 (CH-alkyl), 22.9, 22.8 (2xCH₃-alkyl), 21.2 (CH₂-tocopherol), 20.8 (CH₂-alkyl), 19.9, 19.8 (2xCH₃-alkyl), 13.8, 12.9, 12.0 (3xCH₃-tocopherol); HRMS not detected.

(2R,3R,4S,5R,6S)-2-((Benzoyloxy)methyl)-6-(((R)-2,5,7,8-tetramethyl-2-((4R,8R)-4,8,12-trimethyltridecyl)chroman-6-yl)oxy)tetrahydro-2*H*-pyran-3,4,5-triyl tribenzoate (79)

The benzoyl protected compound **7** (107 mg, 106 μ mol) was dissolved in a MeOH/CH₂Cl₂ mixture (1 mL, 1:1) followed by

the addition of sodium methoxide (30% in MeOH, 2 drops). The mixture was stirred for 6 hours at room temperature. After reaching completion the reaction was quenched with amberlite®, which was subsequently filtered off and washed with MeOH. The solution was concentrated yielding the crude product which was purified first by silica column chromatography to yield the final compound 8 (55 mg, 93 μ mol, 88% yield) as a white solid. ¹H NMR (400 MHz, MeOD) δ 4.51 (d, J = 7.7 Hz, 1H, H-1), 3.72 (dd, J = 11.8, 2.3 Hz, 1H, H-6a), 3.67 (dd, J = 11.7, 4.5 Hz, 1H, H-6b), 3.54 (dd, J = 9.2, 7.8 Hz, 1H, H-2), 3.49 - 3.40 (m, 2H, H-3 and H-4), 3.10 (ddd, J = 9.1, 4.3, 3.1 Hz, 1H, H-5), 2.54 (g, J = 6.2 Hz, 2H, CH₂-tocopherol), 2.19 (s, 3H, CH₃tocopherol), 2.15 (s, 3H, CH₃-tocopherol), 2.04 (s, 3H, CH₃-tocopherol), 1.84 - 1.67 (m, 2H, CH₂-tocopherol), 1.57 - 1.00 (m, 25H, CH₋, CH₂- and CH₃-alkyl), 0.82 (t, J =7.0 Hz, 12H, 4xCH₃-alkyl); 13 C NMR (101 MHz, MeOD) δ 148.7, 146.0, 129.0, 127.2, 123.1, 117.9 (6xC_a-tocopherol), 104.8 (C-1), 76.9 (C-3 or C-4), 76.0 (C-5), 75.3 (C_atocopherol), 74.7 (C-2), 70.8 (C-3 or C-4), 62.3 (C-6), 40.6, 39.7, 37.7 (3xCH₂-alkyl), 33.1 (CH-alkyl), 31.6 (CH₂-tocopherol), 28.3 (CH-tocopherol), 25.1, 24.7 (2xCH₂alkyl), 24.1, 23.9 (2xCH-alkyl), 22.9, 22.8 (2xCH₃-alkyl), 21.4 (CH₂-tocopherol), 21.0 (CH₂-alkyl), 20.0, 19.9, 13.8, 13.0, 12.0 (3xCH₃-tocopherol); HRMS: calcd. for C₃₅H₆₀O₇ [M+NH₄]⁺ 610,46773, found: 610,46832

(2R,3R,4S,5R,6R)-2- $((Benzoyloxy)methyl-^{13}C)$ -6-(((R)-2,5,7,8-tetramethyl-2-((4R,8R)-4,8,12-trimethyltridecyl)chroman-6-yl)oxy)tetrahydro-2*H*-pyran-3,4,5-triyl-2,3,4,5,6- $^{13}C_5$ tribenzoate (80)

The bezoyl protected imidate $^{13}C_6$ glucose donor (Synthesis shown in Chapter 2, 100 mg, 134 µmol) was dissolved in

anhydrous CH_2Cl_2 (2.7 mL) and α -Tocopherol (87 mg, 202 μ mol) was added. The reaction mixture was cooled to $-30\,^{\circ}$ C on activated 4 Å molecular sieves under argon atmosphere. Boron trifluoride etherate (7 μ L, 54 μ mol) was added and stirring was

maintained for 4 and an half hour. After completion the reaction was neutralized with triethylamine (18 μ L) and filtered over celite after which the mixture was evaporated under reduced pressure and purified by silica column chromatography to yield the product **9** (123 mg, 121 μ mol, 90%) as a white solid. 1 H-NMR and 13 C-NMR were in accordance with compound **7** and were not further characterized here; HRMS not detected.

(2R,3S,4S,5R,6R)-2- $(Hydroxymethyl^{-13}C)$ -6-(((R)-2,5,7,8-tetramethyl-2-((4R,8R)-4,8,12-trimethyltridecyl)chroman-6-yl)oxy)tetrahydro-2*H*-pyran-3,4,5-triol-2,3,4,5,6- $^{13}C_5$ (81)

The benzoyl protected compound $\bf 9$ (123 mg, 121 μ mol) was dissolved in a MeOH/CH₂Cl₂ mixture (1.2 mL,

1:1) followed by the addition of sodium methoxide (30% in MeOH, 2 drops). The mixture was stirred for 6 hours at room temperature. After reaching completion the reaction was quenched with amberlite®, which was subsequently filtered off and washed with MeOH. The solution was concentrated yielding the crude product which was purified first by silica column chromatography to yield the final compound 10 (55 mg, 92 μmol, 76% yield) as a white solid. ¹H NMR (400 MHz, DMSO) δ 5.48 (d, J = 4.8 Hz, 1H, OH), 5.02 (d, J = 4.1 Hz, 1H, OH), 4.91 (d, J = 4.8 Hz, 1H, OH), 4.33 (d, J = 7.2 Hz, 1H, H-1), 4.25 (q, J = 5.0 Hz, 1H, OH), 3.58 (d, J = 10.5 Hz, 1H, H-6a), 3.45 – 3.38 (m, 1H, H-6b), 3.30 – 3.23 (m, 1H, H-5), 3.22 – 3.10 (m, 2H, H-3 and H-4), 2.96 - 2.92 (m, 1H, H-2), 2.15 (s, 3H, CH₃-tocopherol), 2.13 (s, 3H, CH₃tocopherol), 1.97 (s, 3H, CH₃-tocopherol), 1.72 (t, J = 7.3 Hz, 2H, CH₂-tocopherol), 1.55 - 0.98 (m, 25H, CH-, CH₂- and CH₃-alkyl), 0.82 (dd, J = 8.6, 6.5 Hz, 12H, 4xCH₂alkyl); 13 C NMR (101 MHz, DMSO) δ 147.4, 146.0, 128.4, 126.6, 121.2, 116.9 (6xC₀tocopherol), 104.8 (dd, J = 46.9, 4.9 Hz, C-1), 76.6 (td, J = 40.6, 38.8, 15.4 Hz, C-2 and C-3 or C-4), 74.4 (C_0 -tocopherol), 74.1 (dd, J = 46.9, 38.8 Hz, C-5), 70.0 (t, J = 40.1 Hz, C-3 or C-4), 61.2 (dt, J = 43.9, 4.0 Hz, C-6), 36.7, 36.7, 36.6 (3xCH₂-alkyl), 32.0 (CHalkyl), 30.3 (CH₂-tocopherol), 27.4 (CH-alkyl), 24.2 (CH₃-alkyl), 23.7, 23.5 (2xCH₂alkyl), 22.6, 22.5 (2xCH₃-alkyl), 20.4 (CH₂-tocopherol), 20.1 (CH₂-alkyl), 19.6 (2xCH₃alkyl), 13.6, 12.7, 11.7 (3xCH₃-tocoherol); HRMS: calcd. for $C_{29}^{13}C_6H_{60}O_7$ [M+NH₄]⁺ 616,48786 found: 616,48838.

Synthesis of clicked fluorogenic substrates 6-TriazoleC16-4MU-8-Glc **43** and 6-TriazoleTMA-4MU-8-Glc **44**.

Substrate **43** was prepared using a copper catalysed click reaction of **42** and hexadecyne with sodium ascorbate and copper sulfate in a mixture of dichloromethane and water followed by an acetyl deprotection using sodium methoxide. The TMA functionalized fluorogenic substrate **44** was synthesized using the same synthetic steps and conditions but instead of using hexadecyne the alkyne **41** was used which was prepared from a simple alkylation step of choline and propargylbromide using sodium hydroxide in acetonitrile to yield **44** quantitatively.

N,N,N-Trimethyl-2-(prop-2-yn-1-yloxy)ethan-1-aminium (41)

acetonitrile (0.2 M). After 30 minutes the solution reached room temperature and propargylbromide (1.18 mL, 10.6 mmol) was added dropwise to the solution. The resulting reaction mixture was reacted under reflux overnight and subsequently filtered concentrated *in vacuo*. The residue was recrystallized from dichloromethane and diethyl ether to obtain *N,N,N*-Trimethyl-2-(prop-2-yn-1-yloxy)ethan-1-aminium (1.36 g, 9.6 mmol, quantitative yield) as an off-white solid. 1 H NMR (500 MHz, MeOD) δ 4.27 (s, 2H, CH₂-CCH), 4.02 – 3.98 (m, 2H, CH₂CH₂N(CH₃)₃), 3.70 – 3.66 (m, 2H, CH₂CH₂N(CH₃)₃), 3.24 (s, 9H, CH₂CH₂N(CH₃)₃); 13 C NMR (126 MHz, MeOD) δ 66.80, 66.77, 66.75 (3xCH₂CH₂N(CH₃)₃), 64.4 (CH₂CH₂N(CH₃)₃), 59.1 (CH₂-CCH), 54.81, 54.78, 54.75 (3xCH₂CH₂N(CH₃)₃); HRMS: not found.

4-Methyl-7-(((2*S*,3*R*,4*S*,5*S*,6*R*)-3,4,5-trihydroxy-6-((4-tetradecyl-1*H*-1,2,3-triazol-1-yl)methyl)tetrahydro-2*H*-pyran-2-yl)oxy)-2*H*-chromen-2-one (43)

then directly diluted with CH₂Cl₂, washed with brine and dried over MgSO₄. The combined organic layer was filtered and concentrated *in vacuo* to give a crude residue which directly deprotected in the next step. The crude sugar was dissolved in a 1:1 mixture of MeOH and CH₂Cl₂ (0.1 M) after which sodium methoxide (30% in MeOH, 1

drop) was added to the solution at room temperature and the mixture was stirred at this temperature for 4 h. After reaching completion, the mixture was quenched with amberlite®, and subsequently filtered off and washed with MeOH. The solution was concentrated in vacuo yielding the crude product which was purified by silica column chromatography to yield the product (31 mg, 53 µmol, 61% over 2 steps) as a white solid. ¹H NMR (400 MHz, MeOD/CDCl₃) δ 7.52 – 7.46 (m, 1H, CH-Um), 7.35 (s, 1H, CH-triazole), 6.76 (d, J = 2.4 Hz, 1H, CH-Um), 6.72 (dd, J = 8.8, 2.5 Hz, 1H, CH-Um), 6.16 (d, J = 1.4 Hz, 1H, CH-Um), 4.91 (d, J = 2.5 Hz, 1H, H-1), 4.91 - 4.86 (m, 1Hm H-6a), 4.39 (dd, J = 14.4, 8.6 Hz, 1H, H-6b), 3.86 – 3.77 (m, 1H, H-5), 3.55 – 3.47 (m, 2H, H-2 and H-4), 3.27 (ddd, J = 9.3, 6.3, 3.0 Hz, 1H, H-3), 2.70 - 2.51 (m, 2H, CH₂-alkyl), 2.41 (d, J = 1.3 Hz, 3H, CH₃-Um), 1.57 - 1.38 (m, 2H, CH_2 -alkyl), 1.19 (d, J = 19.7 Hz, 22H, $11xCH_2$ -alkyl), 0.88 - 0.81(m, 3H, CH₃-alkyl); 13 C NMR (101 MHz, MeOD/CDCl₃) δ 162.3, 160.4, 155.0, 153.9 (4xC_g-Um), 148.7 (C_q-triazole), 126.3 (CH-Um), 123.4 (CH-Triazole), 115.5 (C_q-Um), 113.7, 112.8, 104.7 (3xCH-Um), 100.5 (C-1), 76.6 (C-2 or C-4), 75.3 (C-5), 73.5 (C-2 or C-4), 71.6 (C-3), 51.6 (C-6), 32.3, 31.0, 30.10, 30.08, 30.06, 30.0, 29.80, 29.77, 29.7, 29.6, 25.8, 23.1 (13xCH₂-alkyl), 18.9 (CH₃-Um), 14.3 (CH₃-alkyl); HRMS: calcd. for C₃₂H₄₇N₃O₇ [M+H]⁺: 586.34868, Found: 586.34880.

N,N,N-Trimethyl-2-((1-(((2*R*,3*S*,4*S*,5*R*,6*S*)-3,4,5-trihydroxy-6-((4-methyl-2-oxo-2*H*-chromen-7-yl)oxy)tetrahydro-2*H*-pyran-2-yl)methyl)-1*H*-1,2,3-triazol-4-yl)methoxy)ethan-1-aminium (44)

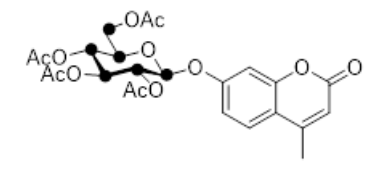
To a biphasic solution of the azide sugar **42** (60 mg, 143 μ mol) and alkyne **41** (61 mg, 429 μ mol) in CH₂Cl₂ and water (0.1 M) was added sodium ascorbate (85 mg, 430 μ mol) and CuSO₄ (69 mg, 430 μ mol). This mixture was stirred vigorously at room temperature for 18 h. Once the reaction was completed, it was diluted with CH₂Cl₂, washed with brine and dried over MgSO₄. The

combined organic layer was filtered and concentrated *in vacuo* to give a crude residue which directly deprotected in the next step. The crude sugar was dissolved in a 1:1 mixture of MeOH and CH_2Cl_2 (0.1 M) after which sodium methoxide (30% in MeOH, 1 drop) was added to the solution at room temperature and the mixture was stirred at this temperature for 4 hours. After reaching completion the mixture was quenched with amberlite®, which was subsequently filtered off and washed with MeOH. The solution was concentrated *in vacuo* yielding the crude product which was purified by silica column chromatography to yield the product (10 mg, 20 μ mol, 40% over 2 steps) as a white solid. 1 H NMR (500 MHz, MeOD) δ 7.94 (s, 1H, CH-Triazole), 7.67 (d, J = 8.8 Hz, 1H,

CH-Um), 6.95 (dd, J = 8.8, 2.4 Hz, 1H, CH-Um), 6.54 (d, J = 2.4 Hz, 1H, CH-Um), 6.22 (d, J = 1.2 Hz, 1H, CH-Um), 5.00 - 4.94 (m, 2H, H-1 and H-6a), 4.74 (d, J = 12.5 Hz, 1H, CHHOCH₂CH₂N(CH₃)₃), 4.66 (d, J = 12.4 Hz, 1H, CHHOCH₂CH₂N(CH₃)₃), 4.53 (dd, J = 14.3, 9.2 Hz, 1H, H-6b), 3.97 (dp, J = 6.4, 3.6 Hz, 2H, CH₂CH₂N(CH₃)₃), 3.95 - 3.89 (m, 1H, H-5), 3.62 - 3.58 (m, 2H, CH₂N(CH₃)₃), 3.55 - 3.46 (m, 2H, H-2 and H-4), 3.35 (m, 1H, H-3), 3.18 (s, 9H, N(CH₃)₃), 2.45 (d, J = 1.2 Hz, 3H, CH₃-Um); ¹³C NMR (126 MHz, MeOD) δ 161.8, 160.3, 154.7, 154.1 (4xC_q-Um), 144.0 (C_q-Triazole), 125.9 (CH-Um), 124.5 (CH-Triazole), 114.8 (C_q-Um), 114.3, 111.7, 102.7 (3xCH-Um), 100.2 (C-1), 76.1 (C-2 or C-4), 74.9 (C-5), 73.3 (C-2 or C-4), 71.4 (C-3), 65.5 (CH₂N(CH₃)₃), 63.8 (CH₂CH₂N(CH₃)₃), 63.5 (CH₂OCH₂CH₂N(CH₃)₃), 53.4, 53.3, 53.3 ((CH₂CH₂N(CH₃)₃), 51.3 (C-6), 17.3 (CH₃-Um); HRMS: calcd. for C₂₄H₃₃N₄O₈⁺ [M+]⁺: 505.22929, Found: 505.22942.

Synthesis of ${}^{13}C_6$ isotope labeled 4MU-8-Glc 83.

$(2R,3R,4S,5R,6S)-2-(Acetoxymethyl-^{13}C)-6-((4-methyl-2-oxo-2$ *H*-chromen-7-yl)oxy)tetrahydro-2*H* $-pyran-3,4,5-triyl-2,3,4,5,6-^{13}C₅ triacetate (82)$

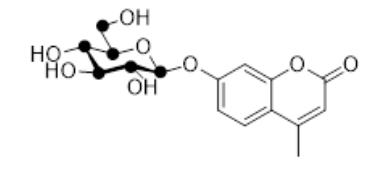


Hydrogen bromide (33% in acetic acid, 5 mL, 30.4 mmol) was added dropwise to **75** (500 mg, 1.28 mmol) in CH_2Cl_2 (5 mL) at 0 °C and was stirred at this temperature for 4 hours. Upon completion ice water (50 mL) was added to the mixture and the aqueous

phase was extracted with CH₂Cl₂ (3x). The combined organic layers were washed with sat. NaHCO₃ (3x) and brine after which the organic layer was dried (MgSO₄), filtered and concentrated under reduced pressure. The crude product was immediately used in the next step without further purification. 4MU (386 mg, 2.19 mmol) was added to a solution of NaOH (83 mg, 2.08 mmol) in water (11 mL). To this solution was added the crude bromide (450 mg, 1.09 mmol) dissolved in acetone (11 mL). The mixture was stirred in the dark overnight at room temperature. After reaching completion the reaction was diluted with CH₂Cl₂ and washed with 1 M NaOH (2x) and brine. The water layers were extracted with CH₂Cl₂ and the combined organic layers were dried (MgSO₄), filtered and concentrated under reduced pressure. The product was purified by silica column chromatography to yield the product 82 (160 mg, 316 μmol, 25% over 2 steps) as a white solid. 1 H NMR (400 MHz, CDCl₃) δ 7.53 (d, J = 8.7 Hz, 1H, CH-Um), 6.97 (d, J = 2.4 Hz, 1H, CH-Um), 6.94 (dd, J = 8.6, 2.4 Hz, 1H, CH-Um), 6.20 (d, J = 1.3 Hz, 1H, CH-Um), 5.39 - 5.27 (m, 2H, H-2 and H-3), 5.24 - 5.13 (m, 2H, H-1 and H-4), 4.31 (dd, J = 12.2, 5.5Hz, 1H, H-6a), 4.22 - 4.16 (m, 1H, H-6b), 3.95 (dd, J = 10.5, 5.0 Hz, 1H, H-5), 2.42 (d, J = 10.5, 5.0 Hz, 1H, H-5), 2.52 (d, J = 10.5, 5.0 Hz, 1H, H-5), 2.42 (d, J = 10.5, 5.0 Hz, 1H, H-5), 2.42 (d, J = 10.5, 5.0 Hz, 1H, H-5), 2.42 (d, J = 10.5, 5.0 Hz, 1H, H-5), 2.52 (d, J = 10.5, 5.0 Hz, 1 1.3 Hz, 3H, CH₃-Um), 2.13 (s, 3H, CH₃-OAc), 2.08 (s, 3H, CH₃-OAc), 2.07 (s, 3H, CH₃-OAc), 2.05 (s, 3H, CH₃-OAc); 13 C NMR (101 MHz, CDCl₃) δ 170.7, 170.2, 169.5, 169.3 (4xC_q-OAc), 276

160.8, 159.2, 154.9, 152.3 (4xC_q-Um), 125.8 (CH-Um), 115.6 (C_q-Um), 114.0, 113.2, 104.0 (3xCH-Um), 98.4 (dt, J = 48.3, 5.0 Hz, C-1), 73.2 – 71.9 (m, C-2 or C-3 and C-5), 70.9 (ddd, J = 48.2, 41.0, 3.7 Hz, C-2 or C-3), 68.1 (td, J = 41.3, 3.8 Hz, C-4), 61.9 (dt, J = 44.6, 4.1 Hz, C-6), 20.8, 20.7, 20.7 (4xCH₃-OAc), 18.7 (CH₃-Um); HRMS: calcd. for C₁₀¹³C₆H₁₈O₈ [M+H]⁺ 513,16983, found: 513,17066.

4-Methyl-7-(((2S,3R,4S,5S,6R)-3,4,5-trihydroxy-6-(hydroxymethyl- 13 C)tetrahydro-2H-pyran-2-yl-2,3,4,5,6- 13 C₅)oxy)-2H-chromen-2-one (83)



The protected sugar **82** (159 mg, 314 μ mol) was dissolved in a MeOH/CH₂Cl₂ mixture (6 mL, 1:1) followed by the addition of sodium methoxide (30% in MeOH, 2 drops). The mixture was stirred for 4 hours at room temperature. After reaching completion the

reaction was quenched with amberlite®, which was subsequently filtered off and washed with MeOH. The solution was concentrated under reduced pressure yielding the crude product which was purified by silica column chromatography to yield the final compound **83** (76 mg, 255 μmol, 72% yield) as a white solid. 1 H NMR (400 MHz, MeOD) δ 7.70 (d, J = 8.8 Hz, 1H, CH-Um), 7.11 (dd, J = 8.8, 2.4 Hz, 1H, CH-Um), 7.06 (d, J = 2.4 Hz, 1H, CH-Um), 6.20 (d, J = 1.3 Hz, 1H, CH-Um), 5.04 (d, J = 7.2 Hz, 1H, H-1), 3.91 (dd, J = 12.0, 2.0 Hz, 1H, H-6a), 3.71 (dd, J = 12.1, 5.6 Hz, 1H, H-6b), 3.56 – 3.46 (m, 3H, H-2, H-5 and H-3 or H-4), 3.44 – 3.37 (m, 1H, H-3 or H-4), 2.45 (d, J = 1.2 Hz, 3H, CH₃-Um); 13 C NMR (101 MHz, MeOD) δ 163.3, 162.0, 156.0, 155.5 (4xCq-Um), 127.3 (CH-Um), 116.0 (Cq-Um), 115.0, 112.9, 105.0 (3xCH-Um), 101.9 (dt, J = 46.9, 4.7 Hz, C-1), 78.9 – 77.0 (m, C-2 and/or C-3, C-4 or C-5), 74.7 (ddd, J = 46.9, 39.2, 2.7 Hz, C-2 or C-3 or C-4 or C-5), 71.2 (td, J = 40.2, 39.3, 2.6 Hz, C-3 or C-4), 62.4 (dt, J = 43.2, 4.3 Hz, C-6), 18.7 (CH₃-Um); HRMS: calcd. for C₁₀¹³C₆H₁₈O₈ [M+H]⁺ 345,12757 found: 345,12797.

6.4 References

- (1) Grille, S.; Zaslawski, A.; Thiele, S.; Plat, J.; Warnecke, D. The Functions of Steryl Glycosides Come to Those Who Wait: Recent Advances in Plants, Fungi, Bacteria and Animals. *Prog. Lipid Res.* **2010**, *49* (3), 262–288.
- (2) Franco, R.; Sánchez-Arias, J. A.; Navarro, G.; Lanciego, J. L. Glucocerebrosidase Mutations and Synucleinopathies. Potential Role of Sterylglucosides and Relevance of Studying Both GBA1 and GBA2 Genes. *Front. Neuroanat.* **2018**, *12* (June), 1–8.
- (3) Schulz, J. D.; Hawkes, E. L.; Shaw, C. A. Cycad Toxins, Helicobacter Pylori and Parkinsonism: Cholesterol Glucosides as the Common Denomenator. *Med. Hypotheses* **2006**, *66* (6), 1222–1226.
- Usuki, S.; Kamitani, T.; Matsuo, Y.; Yu, R. K. Pathobiochemical Effect of Acylated Steryl-β-Glucoside on Aggregation and Cytotoxicity of α-Synuclein. *Neurochem. Res.* **2012**, *37* (6), 1261–1266.
- (5) Van Kampen, J. M.; Baranowski, D. C.; Robertson, H. A.; Shaw, C. A.; Kay, D. G.; Lewis, P. The Progressive BSSG Rat Model of Parkinson's: Recapitulating Multiple Key Features of the Human Disease. *PLoS One* **2015**, *10* (10), 1–26.
- (6) Beutler, E. Grabowski, G. A. Gaucher Disease, in McGraw-Hill (Ed). *Metab. Mol. bases Inherit. Dis.* **2001**, 3635–3668.
- (7) Stoker, T. B.; Torsney, K. M.; Barker, R. A. Pathological Mechanisms and Clinical Aspects of GBA1 Mutation-Associated Parkinson's Disease. *Park. Dis. Pathog. Clin. Asp.* **2018**, 45–64.
- (8) Migdalska-Richards, A.; Daly, L.; Bezard, E.; Schapira, A. H. V. Ambroxol Effects in Glucocerebrosidase and α-Synuclein Transgenic Mice. *Ann. Neurol.* 2016, 80 (5), 766–775.
- (9) Shimamura, M. Structure, Metabolism and Biological Functions of Steryl Glycosides in Mammals. *Biochem. J.* **2020**, *477* (21), 4243–4261.
- (10) Kovganko, N. V; N., K. Z. Sterol Glycosides and Acylgycosides. *Bioorg. Chem.* **1999**, *35* (5), 479–497.
- (11) Akiyama, H.; Sasaki, N.; Hanazawa, S.; Gotoh, M.; Kobayashi, S.; Hirabayashi, Y.; Murakami-Murofushi, K. Novel Sterol Glucosyltransferase in the Animal Tissue and Cultured Cells: Evidence That Glucosylceramide as Glucose Donor. *Biochim. Biophys. Acta Mol. Cell Biol. Lipids* 2011, 1811 (5), 314–322.
- (12) Boer, D. E.; Mirzaian, M.; Ferraz, M. J.; Zwiers, K. C.; Baks, M. V.; Hazeu, M. D.; Ottenhoff, R.; Marques, A. R. A.; Eijer, R.; Roos, J. C. P.; Cox, T. M.; Boot, R. G.; Pannu, N.; Overkleeft, H. S.; Artola, M.; Aerts, J. M. Human Glucocerebrosidase Mediates Formation of Xylosylcholesterol by β-Xylosidase and Transxylosidase Reactions. *Journal of Lipid Research*. 2021, p 100018.
- (13) Akiyama, H.; Ide, M.; Nagatsuka, Y.; Sayano, T.; Nakanishi, E.; Uemura, N.; Yuyama, K.; Yamaguchi, Y.; Kamiguchi, H.; Takahashi, R.; Aerts, J. M. F. G.; Greimel, P.; Hirabayashi, Y. Glucocerebrosidases Catalyse a Transgalactosylation Reaction That Yields a Newly-Identified Brain Sterol Metabolite, Galactosylated Cholesterol. J. Biol. Chem. 2020, 295 (16), 5257–5277.
- (14) Dardis, A.; Michelakakis, H.; Rozenfeld, P.; Fumic, K.; Wagner, J.; Pavan, E.; Fuller, 278

- M.; Revel-Vilk, S.; Hughes, D.; Cox, T.; Aerts, J. Patient Centered Guidelines for the Laboratory Diagnosis of Gaucher Disease Type 1. *Orphanet J. Rare Dis.* **2022**, *17* (1), 1–17.
- (15) van Weely, S.; Brandsma, M.; Strijland, A.; Tager, J. M.; Aerts, J. M. F. G. Demonstration of the Existence of a Second, Non-Lysosomal Glucocerebrosidase That Is Not Deficient in Gaucher Disease. *BBA Mol. Basis Dis.* **1993**, *1181* (1), 55–62.
- (16) Dekker, N.; Voorn-Brouwer, T.; Verhoek, M.; Wennekes, T.; Narayan, R. S.; Speijer, D.; Hollak, C. E. M.; Overkleeft, H. S.; Boot, R. G.; Aerts, J. M. F. G. The Cytosolic β-Glucosidase GBA3 Does Not Influence Type 1 Gaucher Disease Manifestation. *Blood Cells, Mol. Dis.* 2011, 46 (1), 19–26.
- (17) Nyström, L.; Schär, A.; Lampi, A. M. Steryl Glycosides and Acylated Steryl Glycosides in Plant Foods Reflect Unique Sterol Patterns. *Eur. J. Lipid Sci. Technol.* **2012**, *114* (6), 656–669.
- (18) Ostlund, R. E. Phytosterols in Human Nutrition. *Annu. Rev. Nutr.* **2002**, *22*, 533–549.
- (19) Van Kampen, J. M.; Robertson, H. A. The BSSG Rat Model of Parkinson's Disease: Progressing towards a Valid, Predictive Model of Disease. *EPMA J.* **2017**, *8* (3), 261–271.
- (20) Akiyama, H.; Kobayashi, S.; Hirabayashi, Y.; Murakami-Murofushi, K. Cholesterol Glucosylation Is Catalysed by Transglucosylation Reaction of β-Glucosidase 1. *Biochem. Biophys. Res. Commun.* **2013**, *441* (4), 838–843.
- (21) Halima, M. (Ph.D. Thesis 2023, Leiden University). Ginsenosides as Selective Glucocorticoid Drugs: Agonists, Antagonists, and Prodrugs. Https://Hdl.Handle.Net/1887/3620137.
- Ghisaidoobe, A. T.; Van Den Berg, R. J. B. H. N.; Butt, S. S.; Strijland, A.; Donker-Koopman, W. E.; Scheij, S.; Van Den Nieuwendijk, A. M. C. H.; Koomen, G. J.; Van Loevezijn, A.; Leemhuis, M.; Wennekes, T.; Van Der Stelt, M.; Van Der Marel, G. A.; Van Boeckel, C. A. A.; Aerts, J. M. F. G.; Overkleeft, H. S. Identification and Development of Biphenyl Substituted Iminosugars as Improved Dual Glucosylceramide Synthase/Neutral Glucosylceramidase Inhibitors. J. Med. Chem. 2014, 57 (21), 9096–9104.
- (23) Cox, T.; Lachmann, R.; Hollak, C.; Aerts, J.; Van Weely, S.; Hrebícek, M.; Platt, F.; Butters, T.; Dwek, R.; Moyses, C.; Gow, I.; Elstein, D.; Zimran, A. Novel Oral Treatment of Gaucher's Disease with N-Butyldeoxynojirimycin (OGT 918) to Decrease Substrate Biosynthesis. *Lancet* **2000**, *355* (9214), 1481–1485.
- (24) Overkleeft, H. S.; Renkema, G. H.; Neele, J.; Vianello, P.; Hung, I. O.; Strijland, A.; Van Der Burg, A. M.; Koomen, G. J.; Pandit, U. K.; Aerts, J. M. F. G. Generation of Specific Deoxynojirimycin-Type Inhibitors of the Non-Lysosomal Glucosylceramidase. *J. Biol. Chem.* **1998**, *273* (41), 26522–26527.
- (25) Wennekes, T.; Meijer, A. J.; Groen, A. K.; Boot, R. G.; Groener, J. E.; Van Eijk, M.; Ottenhoff, R.; Bijl, N.; Ghauharali, K.; Song, H.; O'Shea, T. J.; Liu, H.; Yew, N.; Copeland, D.; Van Den Berg, R. J.; Van Der Marel, G. A.; Overkleeft, H. S.; Aerts, J. M. Dual-Action Lipophilic Iminosugar Improves Glycemic Control in Obese Rodents by Reduction of Visceral Glycosphingolipids and Buffering of

- Carbohydrate Assimilation. J. Med. Chem. 2010, 53 (2), 689–698.
- (26) Liu, B. (Ph.D. Thesis 2017, Leiden University). Iminosugars as Glucosylceramide Processing Enzymes Inhibitors: Design, Synthesis and Evaluation. Retrieved from Https://Hdl.Handle.Net/1887/57984.
- (27) Su, Q.; Louwerse, M.; Lammers, R. F.; Maurits, E.; Janssen, M.; Boot, R. G.; Borlandelli, V.; Offen, W. A.; Linzel, D.; Schröder, S. P.; Davies, G. J.; Overkleeft, H. S.; Artola, M.; Aerts, J. M. F. G. Selective Labelling of GBA2 in Cells with Fluorescent β-d-Arabinofuranosyl Cyclitol Aziridines. *Chem. Sci.* 2024, 15212–15220.
- (28) Rha, C. S.; Kim, E. R.; Kim, Y. J.; Jung, Y. S.; Kim, D. O.; Park, C. S. Simple and Efficient Production of Highly Soluble Daidzin Glycosides by Amylosucrase from Deinococcus Geothermalis. *J. Agric. Food Chem.* **2019**.
- (29) Lee, Y. S.; Woo, J. Bin; Ryu, S. I.; Moon, S. K.; Han, N. S.; Lee, S. B. Glucosylation of Flavonol and Flavanones by Bacillus Cyclodextrin Glucosyltransferase to Enhance Their Solubility and Stability. *Food Chem.* **2017**, *229*, 75–83.
- (30) Bodel, P.; Dillard, G. M.; Kaplan, S. S.; Malawista, S. E. Anti-Inflammatory Effects of Estradiol on Human Blood Leukocytes. *J Lab Clin Med.* **1972**, *80* (3), 373–384.
- (31) Straub, R. H. The Complex Role of Estrogens in Inflammation. *Endocr. Rev.* **2007**, 28 (5), 521–574.
- (32) Xu, H.; Gouras, G. K.; Greenfield, J. P.; Vincent, B.; Naslund, J.; Mazzarelli, L.; Fried, G.; Jovanovic, J. N.; Seeger, M.; Relkin, N. R.; Liao, F.; Checler, F.; Buxbaum, J. D.; Chait, B. T.; Thinakaran, G.; Sisodia, S. S.; Wang, R.; Greengard, P.; Gandy, S. Estrogen Reduces Neuronal Generation of Alzheimer β-Amyloid Peptides. *Nat. Med.* 1998, 4 (4), 447–451.
- (33) Gold, S. M.; Voskuhl, R. R. Estrogen Treatment in Multiple Sclerosis. *J. Neurol. Sci.* **2009**, *286* (1–2), 99–103.
- (34) Gruber, C. J.; Tschugguel, W.; Schneeberger, C.; Huber, J. C. Production and Actions of Estrogens. *N. Engl. J. Med.* **2002**, *346* (5), 340–352.
- (35) Tucker, J. M.; Townsend, D. M. Alpha-Tocopherol: Roles in Prevention and Therapy of Human Disease. *Biomed. Pharmacother.* **2005**, *59* (7), 380–387.
- (36) Emamzadeh, F. N. Alpha-Synuclein Structure, Functions, and Interactions. *J. Res. Med. Sci.* **2016**, *21* (2).
- (37) Bartels, T.; Choi, J. G.; Selkoe, D. J. Alpha-Synuclein Occurs Physiologically as a Helically Folded Tetramer That Resists Aggregation. *Nature* **2011**, *477* (7362), 107–111.
- (38) Ferreon, A. C. M.; Gambin, Y.; Lemke, E. A.; Deniz, A. A. Interplay of α-Synuclein Binding and Conformational Switching Probed by Single-Molecule Fluorescence. *Proc. Natl. Acad. Sci. U. S. A.* **2009**, *106* (14), 5645–5650.
- (39) Fink, A. L. The Aggregation and Fibrillation of α -Synuclein. *Acc. Chem. Res.* **2006**, 39 (9), 628–634.
- (40) Mahmood, A.; Samad, A.; Bano, S.; Umair, M.; Ajmal, A.; Ilyas, I.; Shah, A. A.; Li, P.; Hu, J. Structural and Dynamics Insights into the GBA Variants Associated with Parkinson's Disease. *J. Biomol. Struct. Dyn.* **2024**, *42* (12), 6256–6268.
- (41) Kim, S.; Yun, S. P.; Lee, S.; Umanah, G. E.; Bandaru, V. V. R.; Yin, X.; Rhee, P.; Karuppagounder, S. S.; Kwon, S. H.; Lee, H.; Mao, X.; Kim, D.; Pandey, A.; Lee, G.;

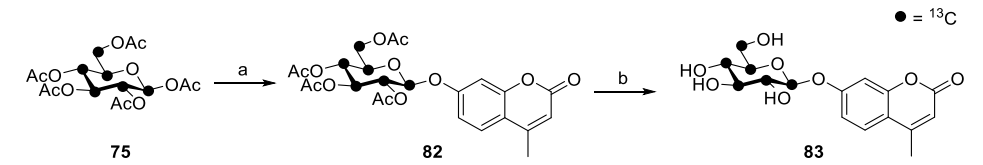
- Dawson, V. L.; Dawson, T. M.; Ko, H. S. GBA1 Deficiency Negatively Affects Physiological α -Synuclein Tetramers and Related Multimers. *Proc. Natl. Acad. Sci. U. S. A.* **2018**, *115* (4), 798–803.
- (42) Sardi, S. P.; Clarke, J.; Viel, C.; Chan, M.; Tamsett, T. J.; Treleaven, C. M.; Bu, J.; Sweet, L.; Passini, M. A.; Dodge, J. C.; Yu, W. H.; Sidman, R. L.; Cheng, S. H.; Shihabuddin, L. S. Augmenting CNS Glucocerebrosidase Activity as a Therapeutic Strategy for Parkinsonism and Other Gaucher-Related Synucleinopathies. *Proc. Natl. Acad. Sci. U. S. A.* 2013, 110 (9), 3537–3542.
- (43) Barkhuizen, M.; Anderson, D. G.; Grobler, A. F. Advances in GBA-Associated Parkinson's Disease Pathology, Presentation and Therapies. *Neurochem. Int.* **2016**, *93*, 6–25.
- (44) Menozzi, E.; Toffoli, M.; Schapira, A. H. V. Targeting the GBA1 Pathway to Slow Parkinson Disease: Insights into Clinical Aspects, Pathogenic Mechanisms and New Therapeutic Avenues. *Pharmacol. Ther.* **2023**, *246*, 108419.
- (45) Mazzulli, J. R.; Xu, Y. H.; Sun, Y.; Knight, A. L.; McLean, P. J.; Caldwell, G. A.; Sidransky, E.; Grabowski, G. A.; Krainc, D. Gaucher Disease Glucocerebrosidase and α-Synuclein Form a Bidirectional Pathogenic Loop in Synucleinopathies. *Cell* **2011**, *146* (1), 37–52.
- (46) Do, J.; McKinney, C.; Sharma, P.; Sidransky, E. Glucocerebrosidase and Its Relevance to Parkinson Disease. *Mol. Neurodegener.* **2019**, *14* (1), 1–16.
- (47) Futerman, A. H.; Hardy, J. Finding Common Ground. Nature 2016, 537, 6–7.
- (48) Marotta, N. P.; Cherwien, C. A.; Abeywardana, T.; Pratt, M. R. O-GlcNAc Modification Prevents Peptide-Dependent Acceleration of α-Synuclein Aggregation. *ChemBioChem* **2012**, *13* (18), 2665–2670.
- (49) Pike, L. J. Lipid Rafts: Bringing Order to Chaos. J. Lipid Res. 2003, 44 (4), 655–667.
- (50) Simons, K.; Toomre, D. Lipid Raft and Signal Transduction. *Nat. Rev. Mol. Cell Biol.* **2000**, *1*.
- (51) Futerman, A. H.; Platt, F. M. The Metabolism of Glucocerebrosides From 1965 to the Present. *Mol. Genet. Metab.* **2017**, *120* (1–2), 22–26.
- (52) García-Sanz, P.; M.F.G. Aerts, J.; Moratalla, R. The Role of Cholesterol in α-Synuclein and Lewy Body Pathology in GBA1 Parkinson's Disease. *Mov. Disord.* **2021**, *36* (5), 1070–1085.
- (53) Farsang, E.; Gaál, V.; Horváth, O.; Bárdos, E.; Horváth, K. Analysis of Non-Ionic Surfactant Triton X-100 Using Hydrophilic Interaction Liquid Chromatography and Mass Spectrometry. *Molecules* **2019**, *24* (7).
- (54) Kim, J. H. (MSc. Thesis 2021, University of the Fraser Valley). Studies Towards Finding Selective Substrates for Human β -Glucosidases. Https://Summit.Sfu.ca/Item/35171.
- (55) Wang, C. H.; Liu, J. H.; Lee, S. C.; Hsiao, C. D.; Wu, W. G. Glycosphingolipid-Facilitated Membrane Insertion and Internalization of Cobra Cardiotoxin: The Sulfatide-cardiotoxin Complex Structure in a Membrane-like Environment Suggests a Lipid-Dependent Cell-Penetrating Mechanism for Membrane Binding Polypeptides. J. Biol. Chem. 2006, 281 (1), 656–667.
- (56) Stults, J. T.; Lai, J.; McCune, S.; Wetzel, R. Simplification of High-Energy Collision Spectra of Peptides by Amino-Terminal Derivatization. *Anal. Chem.* **1993**, *65*

- (13), 1703-1708.
- (57) Vath, J. E.; Biemann, K. Microderivatization of Peptides by Placing a Fixed Positive Charge at the N-Terminus to Modify High Energy Collision Fragmentation. *Int. J. Mass Spectrom. Ion Process.* **1990**, *100* (C), 287–299.
- (58) Mirzaei, H.; Regnier, F. Enhancing Electrospray Ionization Efficiency of Peptides by Derivatization. *Anal. Chem.* **2006**, *78* (12), 4175–4183.
- (59) Liao, P. C.; Huang, Z. H.; Allison, J. Charge Remote Fragmentation of Peptides Following Attachment of a Fixed Positive Charge: A Matrix-Assisted Laser Desorption/Ionization Postsource Decay Study. J. Am. Soc. Mass Spectrom. 1997, 8 (5), 501–509.
- (60) Witte, M. D.; Kallemeijn, W. W.; Aten, J.; Li, K. Y.; Strijland, A.; Donker-koopman, W. E.; Van Den Nieuwendijk, A. M. C. H.; Bleijlevens, B.; Kramer, G.; Florea, B. I. Ultrasensitive in Situ Visualisation of Active Glucocerebrosidase Molecules. *Nat. Chem. Biol.* 2010, 6 (12), 907–913.

6.5 Appendix

Scheme S6.1: Synthesis of Glc-estrone **21**, Glc-estradiol **22** and 13 C₆-Glc-estradiol **23**. Reagents and conditions: a) i. PerOAcGlc, TMSBr, BiBr₃, CH₂Cl₂, 0 °C, 2 h. ii. 4MU, Cs₂CO₃, TBABr, Acetone/H₂O (1:1), rt, 18 h. iii. NaOMe, MeOH/CH₂Cl₂ 1:1, rt, 4 h, 2% over 3 steps. b) i. PerOAcGlc or **75**, TMSBr, BiBr₃, CH₂Cl₂, 0 °C, 2 h. ii. 4MU, Cs₂CO₃, TBABr, acetone/H₂O (1:1), rt, 18 h, **76** = 3% in 2 steps and **77** = 3% in 2 steps c) NaOMe, MeOH/CH₂Cl₂ 1:1, rt, 4 h, **22** = 78%, **23** = 76%.

Scheme S6.2: Synthesis of Glc- α -tocopherol **79** and $^{13}C_6$ -Glc- α -tocopherol **81**. Reagents and conditions: a) $^{12}C_6$ - or $^{13}C_6$ -imidate glucosyl donor, α -tocopherol, BF₃.Et₂O, CH₂Cl₂, - 30 °C, 1 h, **78** and **80** = 90%; b) NaOMe, MeOH/CH₂Cl₂ 1:1, rt, 4 h, **79** = 88%, **81** = 76%.



Scheme S6.3: Synthesis of $^{13}C_6$ -4MU- β -Glc 83. Reagent and conditions: a) i. HBr (33% in AcOH), CH₂Cl₂, 0 °C, 4 h. ii. 4MU, NaOH, TBABr, Acetone/H₂O (1:1), rt, 18 h, 25% (2 steps) b) NaOMe, MeOH/CH₂Cl₂ 1:1, rt,